https://doi.org/10.5194/egusphere-2026-2774
Preprint. Discussion started: 16 June 2026

The marine and coastal hazards of Mediterranean cyclones

Sara Pavan[1], Marco Bajo[1], Francesco Barbariol[1], Alvise Benetazzo[1], Silvio Davison[1], and Christian Ferrarin[1]

[1]CNR - National Research Council of Italy, ISMAR - Institute of Marine Sciences, Venice, Italy

Correspondence: Sara Pavan (sara.pavan@cnr.it)

Abstract. This study aims to contribute to the understanding of marine and coastal hazard due to cyclones in the Mediterranean region, through the reproduction of sea level and wind waves with the use of an unstructured and coupled 2D hydrodynamic-wave modelling system. The modelling system is used to produce a numerical hindcast for the period 1994-2020 which is validated against tide gauges, wave buoys and satellite-borne instruments. The sea level and wave results are analysed for 2483 Mediterranean cyclones detected through a meteorological approach based on a composite cyclone detection and tracking method. We study which portion of extreme values (i.e. values exceeding the 99^{th} percentile) of storm surge and significant wave height is associated to Mediterranean cyclones and we find that in the Mediterranean basin, extreme waves are more frequently associated to cyclones than extreme storm surge. Indeed, more than 50% of extreme significant wave heights of the hindcast is associated to waves generated by cyclones in most of the Mediterranean basin. The percentage is higher than 75% in the Western Adriatic basin and in some sub-regions of the Ionian-Meridional basin, as well as in the northwestern part of the Aegean Sea. For storm surge we find that more than 50% of extremes values are linked to cyclones in the Western Mediterranean basin, in most of the Thyrrenian and the Ionian-Meridional basin, and in the Western Adriatic Sea. On the contrary, less than 50% of extreme values of storm surge are associated to cyclones in the Northern and Eastern Adriatic basin, in the Ligurian Sea and in the Levantine-Aegean basin. The cyclone hazard is then evaluated through selected indicators, including peak values of storm surge and significant wave height, as well as the storm erosion potential index and the total storm wave energy which are integrated indices suitable to indicate cyclones intensity. The spatial distribution of the 99^{th} percentile of all hazard parameters shows that the regions characterized by high hazard values vary depending on the parameter considered. In case of maximum significant wave height and total storm wave energy, the highest values are reached in the Western Mediterranean Sea, in the open sea area between the Balearic Islands and Sardinia. In case of maximum storm surge and storm erosion power index, the highest values are observed in the Northern Adriatic basin while the Western Mediterranean is characterized by moderate values. Despite some common patterns between hazard parameters in the Mediterranean basin, the analysis of their relationships stress that there is not an high correlation among most of them. Through some case studies we show that these parameters provide complementary information enabling a more comprehensive overview of cyclone hazard.

1 Introduction

The Mediterranean basin (MB) is a region of high cultural and landscape richness heavily impacted by human activity and represents a focal area for climate change studies (Chiggiato et al., 2023; Lionello et al., 2023). The frequency of marine ex-

https://doi.org/10.5194/egusphere-2026-2774
Preprint. Discussion started: 16 June 2026

treme events and related coastal impacts, including storm tides, coastal flooding and severe sea states, is likely to be altered due to global warming and sea level rise, which may severely threaten the coastal environment and economies (Tuel and Elthair, 2020; Ali et al., 2022). According to several authors (Jansa et al., 2014; Lionello et al., 2019; Flaounas et al., 2022; Portal et al., 2024; Rousseau-Rizzi et al., 2024; Khodayar et al., 2025), many of the meteo-marine hazards that affect the region, including storm surges, extreme waves, heavy rainfall and flash floods, landslides, windstorms, and even compound events are caused by cyclones. Several intense cyclones affected the MB in the last decades showing important economic and social consequences on communities living in coastal areas (Khodayar et al., 2025). In addition, wave storminess, storm surge and sea level rise are the more direct and robust climate indicators for the state of coastal areas, for erosion and flooding (Sánchez-Arcilla et al., 2016). For these reasons, it is crucial to better understand and quantify the marine and coastal hazards of cyclones in the Mediterranean area.

Mediterranean cyclones are mostly developed by baroclinic instability and affected by diabatic processes similarly to other extratropical cyclones in the mid-latitude storm track (Flaounas et al., 2022). In addition, subtropical or even tropical-like storms, called medicanes, can develop in the MB (Miglietta et al., 2025). Sea storms induced by Mediterranean cyclones are usually detected through the analysis of significant wave height (H_s) or water levels data. Most of the time only one parameter is used for storm detection and H_s is the most popular one (Dolan and Davis, 1992; Boccotti, 2000; Fedele and Arena, 2010; Ojeda et al., 2017; Lira-Loarca et al., 2020). Indeed, during extremes conditions waves drive coastal erosion and flooding (Komar, 1983), playing a key role in the extreme water levels (Melet et al., 2018; Toomey et al., 2022b). On the other hand, also water level records from tide gauges can be used to storm detection and to compute an index for storm erosion potential (Zhang et al., 2001). Cohn et al. (2019) show that in the Pacific Northwest of the United States high still water levels, caused by storm surge or spring tides, have a greater potential to produce dune erosion than the largest wave energy (Dominguez et al., 2024).

Once cyclones are detected, they can be studied to assess potential coastal hazard, which is evaluated in literature through the analysis of wind waves and storm surges (Toomey et al., 2022a; Leijnse et al., 2022; Ferrarin et al., 2023) but also through indices like the Total Storm Wave Energy (TSWE) (Amarouche and Akpınar, 2021; Amarouche et al., 2022), the Storm Power Index (SPI) (Anfuso et al., 2016; Lira-Loarca et al., 2022; Amarouche et al., 2022) and the Storm Erosion Potential Index (SEPI) (Fenster and Dominguez, 2022; Dominguez et al., 2024). These indices are also used as intensity variables for storm classification (Dolan and Davis, 1992; Zhang et al., 2001; Molina et al., 2019).

Coastal hazard assessment can be investigated using in-situ data; however, numerical hindcasts represent a valuable alternative, as they offer the possibility to retreive waves and storm surge data in past periods with broader spatial coverage. In the last decades, several hindcasts have been produced for the Mediterranean Sea (Donatini et al., 2015; Mentaschi et al., 2015; Barbariol et al., 2021; Vannucchi et al., 2021; Elshinnawy and Antolínez, 2023). Most of these works only consider wind waves and the meteorological forcing is obtained from global atmospheric reanalysis (e.g. ERA5), non-hydrostatic mesoscale models (e.g.WRF-ARW) or a downscaling. Storm surges modelled through barotropic models in MB are analysed in Marcos et al. (2009); Conte and Lionello (2013); Makris et al. (2023) through hindcasts or future climate scenarios. All these works help in

https://doi.org/10.5194/egusphere-2026-2774
Preprint. Discussion started: 16 June 2026

understanding and characterizing marine extreme conditions but the link with cyclones is not specifically investigated.

The main purpose of this study is to characterize the marine and coastal hazards associated with Mediterranean cyclones over a 27-year period by producing a coupled hydrodynamic–wave hindcast and applying a composite track method for cyclone detection based on atmospheric variables, proposed by Flaounas et al. (2023). The hazard assessment is performed considering different parameters: the cyclone duration, the cyclone influence area, the maximum significant wave height and storm surge, the Total Storm Wave Energy and the Storm Erosion Potential Index. Finally, a deeper analysis of the hazard is performed for some specific cyclones linking the events dynamics to the obtained results for hazard estimation.

2 Methods

2.1 The coupled modelling system

In this study, we use an unstructured and coupled hydrodynamic and wave modelling system to simulate past sea conditions in the whole Mediterranean Sea. The hydrodynamic core is based on the System of HydrodYnamic Finite Element Modules (SHYFEM, Umgiesser et al. (2022)) code, an open-source unstructured ocean model for simulating hydrodynamics and transport processes at very high resolution (https://github.com/georgu/shyfemcm-ismar). The model solves the shallow-water equations in their formulations with levels and transports using a finite element numerical method and semi-implicit time stepping. The model has been already applied to simulate the hydrodynamics in the Mediterranean Sea (Ferrarin et al., 2013, 2018), in the Adriatic Sea (Bellafiore et al., 2018; Bajo et al., 2019; Ferrarin et al., 2019, 2021), and in several coastal systems (see Umgiesser et al. (2022) and references therein). For the astronomical tide computation, the model calculates the equilibrium tidal potential and load tides and uses these quantities to force the free surface (Kantha, 1995). Four semi-diurnal (M2, S2, N2, K2), four diurnal (K1, O1, P1, Q1) and four long-term constituents (Mf, Mm, Ssa, MSm) are considered. In this work, we do not consider baroclinic processes which, in a first approximation, do not affect sea-level variations in the storm surge frequency range. The Coriolis term is included in the equations to consider the rotating frame. The drag coefficients used to model the wind stresses in the momentum equations are variable in space and in time; they are calculated thanks to the coupling with waves.

The wave model, WAVEWATCH III (WW3, [WW3DG] (2019)), is a third-generation spectral wave model which is open source. It solves the random phase spectral action density balance equation for wavenumber-direction spectra over regular and unstructured grids. Source terms for physical processes include parameterizations for wave growth due to the actions of wind, exact and parametrized forms accounting for nonlinear resonant wave-wave interactions, scattering due to wave-bottom interactions, triad interactions, and dissipation due to whitecapping, bottom friction and surf-breaking [WW3DG] (2019). We have used the highest-level implementation of WW3 based on the multigrid driver that allows coupling the unstructured grid type with SHYFEM. The package ST4 is used for the input wind-wave interaction term and the dissipation white-capping term.

SHYFEM and WW3 are coupled based on a so-called “hard coupling”, e.g. binding the models directly in the source code without any external coupling library. The benefit is minimal memory usage and very limited code changes in both models.

https://doi.org/10.5194/egusphere-2026-2774
Preprint. Discussion started: 16 June 2026

Since both models use the same computational grid there is no need for spatial interpolation and the communication is done via global arrays that are assembled at the coupling interval between both models.
The considered interactions between waves, surge and tides are: (1) the contribution of waves to the total water levels and currents through the gradients of the radiation stress induced by waves computed using the theory of Longuet-Higgins and Steward (1964); (2) the effect of the wave on the surface roughness and therefore on the wind drag; (3) the influence of tides, storm surge and currents on the wave propagation affecting the refraction, shoaling and breaking processes. The two numerical models exchange the following variables that are needed to simulate the current-wave interaction:

- from SHYFEM to WW3: water level, water currents;
- from WW3 to SHYFEM: significant wave height, mean wave period, peak wave period, mean wave direction, radiation stress, wave pressure, sea surface roughness.

2.1.1 Model set-up

The hydrodynamic and wave numerical computation is performed on a spatial domain that represents the Mediterranean Sea using an unstructured grid consisting of about 163.000 triangular elements. The application of triangular unstructured grids in both the hydrodynamic and wave models has the advantage of describing more accurately complicated bathymetry and irregular boundaries in shallow water areas. It can also solve the combined large-scale oceanic and small-scale coastal dynamics in the same discrete domain by subdividing the basin into triangles varying in form and size. The resolution of the elements varies from 10 km in the open sea to 500 m near the coast (Fig. 1). The model bathymetry over the Mediterranean Sea is obtained by a bilinear interpolation on the model grid of the European Marine Observation and Data Network dataset (EMODnet Bathymetry Consortium, 2022).

To reproduce the past sea conditions over the period 1994-2020, the ocean simulations were forced by the wind and the mean sea level pressure (MSLP) fields from the meteorological Copernicus European Regional ReAnalysis (CERRA, Schimanke et al. (2021), https://climate.copernicus.eu/copernicus-regional-reanalysis-europe-cerra). CERRA is a pan-European reanalysis dataset with horizontal resolution of 5.5 km and hourly data, forced by the ERA5 global reanalysis (31 km resolution and three-hourly data, Hersbach et al. (2020)). The SHYFEM hydrodynamic model was forced at the lateral boundary of the Atlantic Ocean (off the Gibraltar Strait) with the sea surface height above the geoid from the Atlantic-Iberian Biscay Irish Ocean Physics Reanalysis made available via the E.U. Copernicus Marine Service Information (https://doi.org/10.48670/moi-00029; accessed on 14-Jun-2024). Velocities from the same model (Atlantic-Iberian Biscay Irish Ocean Physics Reanalysis) are also considered through a nudging scheme with a relaxation time equal to 600 s. No waves conditions were prescribed on the open boundary for the wave model.

Simulations cover the period from 01/1994 to 12/2020 with a spin-up period of 1 month. A variable time step, based on a CFL condition with CFL=0.9 (necessary for the explicit part of the scheme), is set for the SHYFEM model with a time

https://doi.org/10.5194/egusphere-2026-2774
Preprint. Discussion started: 16 June 2026

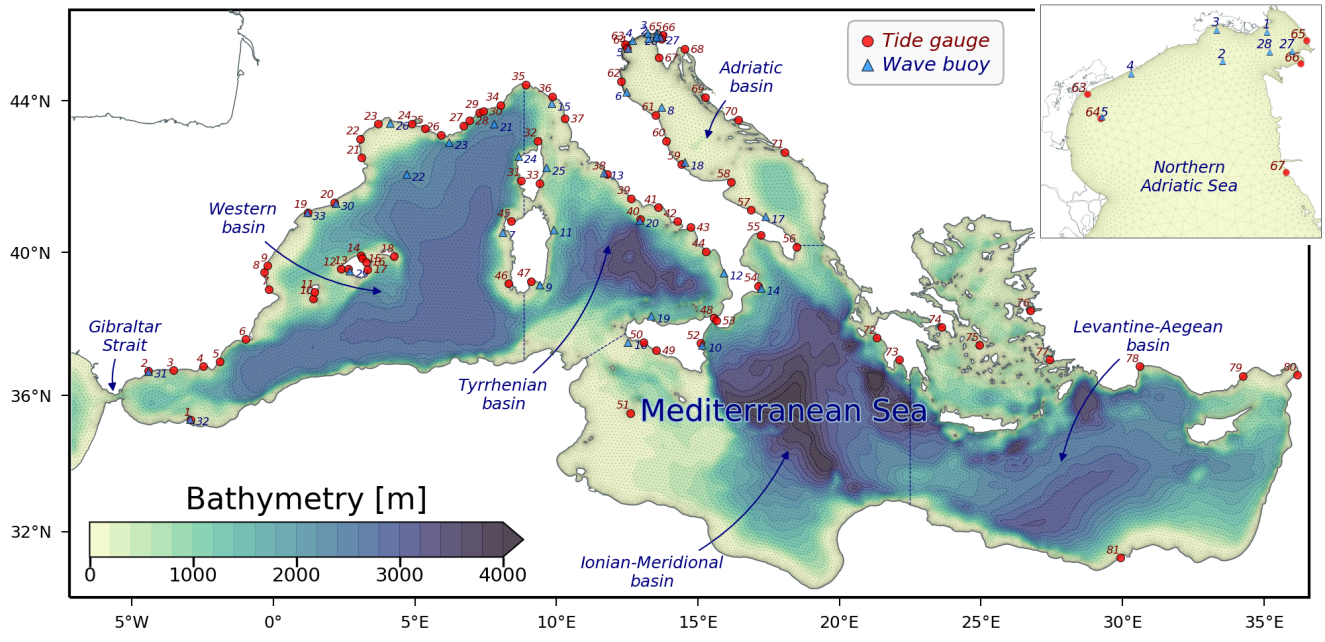

Figure 1. Unstructured numerical grid and bathymetry of the hydrodynamic and wave models with indicated the position of the validation tide gauges (red dots) and wave buoys (blue triangle). The sub-basins considered for the analysis purposes of this paper are separated by dashed blue lines.

step synchronisation every 300 s. A global time step equal to 300 s is used for the wave model. Hourly outputs are set for hydrodynamics variables (sea levels and velocities) and waves (significant wave height, period and direction).

2.2 Cyclone identification and cyclone influence area

When studying cyclones and storms in oceans or coastal waters, it is common to identify the events and to compute their duration using thresholds based on ocean variables (e.g. significant wave height or water level) at specific locations, as explained in Boccotti (2000); Molina et al. (2019); Amarouche et al. (2022); Fenster and Dominguez (2022). In general, threshold values can be fixed according to specific characteristics of the region where storms are studied, based on field evidence (see Dolan and Davis (1992)) or determined using long-term data series (see Amarouche et al. (2022)). In addition, thresholds must often be exceeded for a certain time interval, i.e. a minimum storm duration is fixed (Dolan and Davis, 1992; Anfuso et al., 2016).

Cyclones are, at their core, meteorological phenomena known to induce extreme sea states and sea levels via the direct action of wind and MSLP on the sea surface (Pugh and Woodworth, 2014). For these reasons, to characterize the marine and coastal hazard of Mediterranean cyclones, we choose an event identification method based on a meteorological definition rather than a method based on the threshold analysis of ocean variables. In this work cyclone track and duration are defined according to

https://doi.org/10.5194/egusphere-2026-2774
Preprint. Discussion started: 16 June 2026

Flaounas et al. (2023) by using a composite cyclone track approach based on different detection and tracking methods. Ten different tracking methods are considered in their work and different datasets containing the composite tracks are proposed and ranked according to their confidence level, defined by the number of contributing cyclone detection methods. The main advantage is that the method is the result of the agreement of more than one criteria and it produces cyclone tracks with physically meaningful and distinctive life stages (Flaounas et al., 2023). Lower is the confidence level, higher is the number of identified cyclones and of bogus tracks (i.e. false positives or artifact); higher is the confidence level, lower is the number of identified cyclones but they are generally more intense (deeper and well-organized) systems. In this study, we select composite tracks with a confidence level equal to 5 (called TRACKS CL5), suggested by Flaounas et al. (2023) and also used in Givon et al. (2024) to classify Mediterranean cyclones. Confidence level equal to 5 means that track points are captured by at least five different methods of cyclone tracking and detection. The dataset contains 2483 cyclones in the period from 1994 to 2020 and the average number of tracks per year is about 95 which is sufficient for climatological studies (Flaounas et al., 2023) and corresponds to the mean annual number of cyclones reported in other studies (Flaounas et al., 2022; Doiteau et al., 2024). Cyclone tracks are detected in a larger rectangular domain (20–50° N and 20° W–45° E, see the red box in Fig. 2a) where the MB is enclosed. For each cyclone of Flaounas et al. (2023), the dataset provides an index to identify the cyclone, coordinates in longitude and latitude of the track points, date (year-month-day-hour) and lowest MSLP value within a 2.5° radius from the geographical coordinates of the track point.

To study the cyclone hazard related to the ocean component, we associate to the track a time-variant cyclone influence area instead of considering the whole MB, in which other atmospheric events can occur at the same time. The cyclone influence area is computed for every track point using the wind data provided by the CERRA since the 10 m wind field is the predominant meteorological forcing for waves and storm surge in the Mediterranean Sea. The method to compute the cyclone influence area is inspired by the work of Pérez-Alarcón et al. (2021) where the cyclone size is computed for tropical cyclones in the Atlantic and Pacific basins, using radial wind profiles and applying a wind threshold of $2\,\mathrm{m\,s^{-1}}$. The same wind threshold is used in John A. Knaff and Molenar (2014) to estimate the tropical cyclone size, defined as the radius of where the tropical cyclone wind field is indistinguishable from the background flow in a climatological environment.

In this work we use the same $2\,\mathrm{m\,s^{-1}}$ threshold and wind data over the land are masked, considering a buffer zone for the transition between the sea and the land. For every cyclone track point, wind data are interpolated along 36 radial directions (every 10°) and the maximum distance (and the relative coordinates) with wind velocity larger than $2\,\mathrm{m\,s^{-1}}$ is tracked. This step creates a first approximation of the hourly polygon representing an influence area, which is often very irregular, due to the peculiar orography of the MB. To strengthen the method and increase the polygon regularity, the final hourly polygon is obtained tracing the concave hull of the polygons' coordinates (computed in the previous step) belonging to the time interval (actual time – 4 hours, actual time + 4 hours). In order to obtain one value per event, for each cyclone we consider a time average of the hourly influence area (i.e., the mean cyclone influence area, MCIA).

https://doi.org/10.5194/egusphere-2026-2774
Preprint. Discussion started: 16 June 2026

2.3 Hazard estimation

The numerical results of the hindcast are used to estimate the coastal and marine hazards which are studied within the cyclone influence area. We choose to characterize the hazard according to the following parameters: the maximum storm surge, the maximum significant wave height, the storm erosion power index and the total storm wave energy.

We firstly analyse the storm surge and the significant wave height using statistical tools applied to the whole model hindcast and to the cyclones subset. For each cyclone we compute the maximum of storm surge and of significant wave height in space (over the cyclone influence area) and in time (for the cyclone duration), retaining one value per cyclone. The significant wave height is directly retreived from the hindcast, while the storm surge is obtained through tha analysis of the hindcasted sea levels. In this study, the average duration of cyclones is about 3 days but other phenomena can influence the sea level variations at larger scales. For this reason, the moving monthly average of the water level height is subtracted to the residual sea level value, which is equal to the difference between the sea level and the tidal level. The storm surge (S) can thus be defined as:

$$S(t) = Z(t) - T(t) - \mu_{month}(t) \tag{1}$$

where Z(t) is the simulated water level height, T(t) is the astronomic tidal levels and $\mu_{month}(t)$ is the centred moving monthly average. The tidal levels are based on harmonic analysis which considers four semi-diurnal (M2, S2, N2, K2), four diurnal (K1, O1, P1, Q1) and four long-term constituents (Mf, Mm, Ssa, MSm). The monthly average is computed as:

$$\mu_{month}(t) = \frac{1}{k} \sum_{i=-m_1}^{m_1} Z(t+i) \tag{2}$$

where k = m_1 + m_1 + 1 is the size of the moving monthly average (29 days), expressed in hours and m_1 is the integer number of hours before/after the actual time (14 days X 24 hours/day).

The storm erosion power index (SEPI) has been introduced by Zhang et al. (2001) and incorporates storm tide effects to characterize the potential erosion of sandy beaches. It is based on the analysis of sea levels and storm surges which are considered as a proxy of erosion when two thresholds are overpassed: the mean high higher water (MHHW) for the sea levels and the double of the standard deviation (2SD) of storm surge height for the storm tide levels. The SEPI magnitude is expressed as follows:

$$SEPI_i = \sum_{t=0}^{t_D} S_{2SD}(t) Z_{MHHW}(t) \Delta t \tag{3}$$

where Δt is the time interval (1h in this work) and t_D is the storm duration; the subscript i states that is evaluated at point i. Z_{MHHW}(t) is the water level ($Z(t)$) above the mean higher high water ($\overline{MHHW}$), defined as:

$$Z_{MHHW}(t) = \begin{cases} Z(t), & Z(t) \geq \overline{MHHW} \\ 0, & Z(t) < \overline{MHHW} \end{cases} \tag{4}$$

https://doi.org/10.5194/egusphere-2026-2774
Preprint. Discussion started: 16 June 2026

$S_{2SD}(t)$ is the storm surge ($S(t)$) above the threshold of 2 standard deviations of storm surge, σ_s:

$$S_{2SD}(t) = \begin{cases} S(t), & S(t) \geq 2\sigma_s \\ 0, & S(t) < 2\sigma_s \end{cases} \quad (5)$$

This index has been mainly applied to characterize the storms magnitude along the US coasts, using hourly water level records tide gauges (Zhang et al., 2001; Fenster and Dominguez, 2022; Dominguez et al., 2024). It has been initially proposed to quantify erosion potential of sandy beaches but it can be considered as a more general storm magnitude indicator and for this reason, in this work, it is computed on the whole cyclone influence area and not only in coastal locations. To assign a SEPI value to every cyclone track, we calculate the spatial average over the cyclone influence area of the product of S_{2SD} and Z_{MHHW} ($\overline{S_{2SD} Z_{MHHW}}$). So, the SEPI formula becomes as follows:

$$SEPI = \sum_{t=0}^{t_D} \overline{S_{2SD}(t) Z_{MHHW}(t)} \Delta t \quad (6)$$

The cyclone duration (t_d) is chosen according to the composite track TRACKS CL5.

The total storm wave energy (TSWE) is obtained by integrating the wave power contribution of each sea state over the storm duration. Initially proposed by Arena et al. (2015) to evaluate the energy of storms for performance estimations of a wave energy converter, was then used as parameter to classify and characterize storms (Molina et al., 2019; Amarouche and Akpınar, 2021; Amarouche et al., 2022). The TSWE is defined at point i as (Amarouche et al., 2022):

$$TSWE_i = \int_{t_0}^{t_d} P_w(t) dt \quad (7)$$

Where P_w is the wave power, computed as:

$$P_w = \frac{\rho g^2}{64\pi} H_s^2 T_e \quad (8)$$

With ρ the water density and T_e the energy period (see [WW3DG] (2019)). In this study the storm duration (t_d) over which the wave energy flux is integrated is intrinsically defined by the composite track TRACKS CL5. The wave energy flux is computed only for points belonging to the cyclone influence area. This means that an hourly wave mean power is computed considering the average value ($\overline{P_w}$) obtained from all the points in the cyclone influence area for that hour. The formula is then adapted as follows:

$$TSWE = \int_{t_0}^{t_d} \overline{P_w}(t) dt \quad (9)$$

In Table 1, the selected parameters to describe the marine and coastal cyclone hazard are summarized. The duration and the mean cyclone influence area are derived from the atmospheric analysis: the first one is given by the cyclone track alghoritm and

https://doi.org/10.5194/egusphere-2026-2774
Preprint. Discussion started: 16 June 2026

the second one is computed from wind data. The latter is expressed in terms of the fraction of the Mediterranean Sea surface influenced by the event. The maximum of H_s and S are obtained through the analysis of the tide-surge-wave model results and they are istantaneous and local values. SEPI and TSWE are instead space and time integrated values. Then, we can distinguish between parameters related to waves, such as max(H_s) and TSWE, and parameters related to water levels, such as max(S) and SEPI.

Table 1. List of parameters to characterize the cyclones.

Measure	Unit	Origin	Type
Duration	h	from atmospheric variables	
Mean cyclone influence area	%	from atmospheric variables	time averaged
Max(S)	m	from hydrodynamics	istantaneous and local
Max(H_s)	m	from waves	istantaneous and local
SEPI	m^2 h	from hydrodynamics	space and time integrated
TSWE	Wh m^{-1}	from waves	space and time integrated

3 Results

In this section, the validation of the numerical model is first presented. A wind assessment is performed to ensure the accuracy of the meteorological forcing. Then, the sea level heights and the significant wave heights are evaluated. After the validation of the numerical hindcast, results connected to the atmospheric input data (e.g. density of cyclones track, duration) and cyclones hazard are presented. In this work we use the term extreme (e.g. extreme values, extreme data) referring to those values that are larger than the threshold defined by 99^{th} percentile.

3.1 Model validation

Validation of hindcasted waves and levels is a necessary step which ensures that numerical results are suitable to study the coastal and marine hazards of cyclones in the Mediterranean Sea. The performance of the ocean modelling system is evaluated by comparing the simulated water level and significant wave height with observations collected by tide gauges, wave buoys, and satellite-borne instruments.

In this work, we consider the centered root mean square error (CRMSE), the difference between the mean of simulation results and observations (BIAS), the Pearson cross-correlation coefficient between model results and observations (CC) and the slope of the linear regression best-fit line (SLOPE) as the metrics for measuring the accuracy of the numerical results in representing the sea level and wave variability.

https://doi.org/10.5194/egusphere-2026-2774
Preprint. Discussion started: 16 June 2026

3.1.1 Wind speed assessment

It is well known that most of the uncertainty associated with the simulation of sea storms resides in atmospheric forcing and in particular in wind data. We verify the accuracy of the CERRA reanalysis wind fields against satellite-derived data and the global ERA5 dataset. Satellite data cover the period 2002-2020 and the following satellite missions are considered: ENVISAT (05/2002-04/2012), CryoSat-2 (07/2010-ongoing), Jason-3 (02/2016-ongoing). The added value of the CERRA forcing with respect to the ERA5 global reanalysis product is expected to come with a higher horizontal resolution that permits the usage of a better description of the model topography and physiographic data, and the assimilation of more surface observations. The comparison between CERRA and ERA5 datasets (Fig. S1 in the Supplement) highlights that CERRA overcomes the general ERA5 wind underestimation, indeed the accuracy is higher for CERRA data that has a BIAS of -0.18 $\mathrm{m\,s^{-1}}$ and a CRMSE of 1.35 $\mathrm{m\,s^{-1}}$, compared to a BIAS of -1.02 $\mathrm{m\,s^{-1}}$ and a CRMSE of 2.19 $\mathrm{m\,s^{-1}}$ for ERA5 data. In addition, for CERRA data there is a better correlation between reanalysis data and satellite data, with a slope that approches unity.

3.1.2 Sea level assessment

The Mediterranean Sea is well monitored by several meteo-marine stations, with the highest concentration in the northern regions. Hourly data from 81 tide gauges (red dots in Fig. 1) were considered to validate the model. Data were retrieved from the GESLA3 dataset (Haigh et al., 2023), the tide gauge monitoring network of the Italian Environmental Protection Agency (https://www.mareografico.it/), the regional agency for environmental protection for the Region of Emilia-Romagna (https://www.arpae.it/), the E.U. Copernicus Marine Service (https://marine.copernicus.eu/) and the Acqua Alta oceanographic tower (AAOT; Pomaro et al. (2017)) located in the Northern Adriatic Sea, 15 km offshore the Venetian littoral (marked as tide gauge 63 in Fig. 1). Tide gauges data globally cover the period 1994-2020 and availability increases with time: less than 20 stations are available from 1994 to 1998 while more than 40 stations are available after 2004 (e.g. more than 60 stations for the period 2012-2015).

The accuracy metrics mentioned above are computed on the sea level anomalies (i.e. removing the mean from observations and simulations in order to have data series with zero average). Table 2 shows the average of the errors for the sub-basins of the Mediterranean, illustrated in Fig. 1. Higher values of CC are obtained in the Adriatic basin while lower values are shown in the Ionian-Meridional and Levantine-Aegean basin. We remark that both the Ionian-Meridional basin and the Levantine-Aegean basin have few stations compared to the other sub-basin (holding more than 70% of the stations) and in addition the period of data availability is shorter. For most of the sub-basins except for the Adriatic, the slope is lower than 1 indicating a lower model variability with respect to the observations variability and a systematic underestimation which is a common problem in numerical modelling of the Mediterranean Sea (see Ferrarin et al. (2013)). The latter can be related to several factors like the numerical diffusion and the spatial resolution, the low accuracy of the wind input data, the underestimation of some non-linear effects (e.g. in the coupling between waves and hydrodynamics). The CRMSE varies between 8 and 11 cm: the higher value (11 cm) is obtained in the Adriatic basin, while the Ionian-Meridional basin shows the lowest error equal to 8 cm. Considering all levels and averaging over all sub-basins, the CRMSE is 0.09 m, the CC is 0.77 and the Slope is 0.92. Additionally, the

https://doi.org/10.5194/egusphere-2026-2774
Preprint. Discussion started: 16 June 2026

Table 2. Statistical analysis of simulated sea levels at the tide gauge stations in terms of CRMSE, CC and Slope. Statistics are reported as average values over the different Mediterranean sub-basins.

Sub-basin	CRMSE [m]	CC [/]	Slope [/]
Western	0.09	0.77	0.96
Tyrrhenian	0.09	0.80	0.98
Adriatic	0.11	0.87	1.05
Ionian-Meridional	0.08	0.73	0.87
Levantine-Aegean	0.10	0.70	0.72

correspondence between simulations and observations has been investigated in detail for one station of each sub-basin having the longest period of data availability. Selected stations are: Malaga for the Western basin, Palinuro for the Thyrrenian basin, AAOT for the Adriatic basin, Crotone for the Ionian-Meridional basin, Mentes for the Levantine-Aegean basin (respectively station number 2, 44, 54, 64 and 76 in Fig. 1). Results are shown in Fig. S2 in the Supplement and confirm the values shown in Table 2 indicating a general underestimation of high sea level values, except for the Adriatic where the model tends to slightly overestimate the sea surface elevation.

3.1.3 Wave assessment

To validate the model, significant wave height from 33 wave buoys (blue triangles in Fig. 1) and along-track satellite data (Piollé et al., 2022) derived from multiple satellite missions passing over the Mediterranean Sea were considered. Buoys data were retreived from the monitoring system of the Civil Protection of the Region Friuli Venezia Giulia (https://www.protezionecivile.fvg.it/), the national wave buoy network of the Italian Environmental Protection Agency (ISPRA, https://www.mareografico.it/), the regional agency for environmental protection for the Region of Emilia-Romagna (https://www.arpae.it/), the E.U. Copernicus Marine Service (https://marine.copernicus.eu/) and the Acqua Alta oceanographic tower (AAOT; Pomaro et al. (2017)). Satellite data cover the period from 01/2002 to 12/2018 and the satellite missions are the following: ENVISAT (05/2002-04/2012), CryoSat-2 (07/2010-ongoing), Jason-1 (01/2002-06/2013), Jason-2 (07/2008-10/2019), Jason-3 (02/2016-ongoing), SARAL (03/2013-ongoing), Sentinel-3A (03/2016-ongoing).

Standard error metrics are computed for every wave buoy and every co-located point in case of satellite data. They are grouped and averaged over sub-basins of Mediterranean, as shown in Table 3. For both satellite data and in-situ measurements we find high and similar values of CC (≥ 0.87 in each sub-basin) and biases are negligible ($< 0.08\,\mathrm{m}$). More differences are observed in the CRMSE which is higher for satellite data than for in-situ observations. Taylor diagrams and diagrams showing BIAS-CRMSE (Fig. S3 in the Supplement) stress that for most of the buoys/satellites the model variability is slightly higher than the observations variability ($\sigma_{sim} > \sigma_{obs}$).

Overall, there is a good agreement between numerical results and observations and validation results are comparable to those obtained for other hindcast (Lira-Loarca et al., 2022; Barbariol et al., 2021; Elshinnawy and Antolínez, 2023).

https://doi.org/10.5194/egusphere-2026-2774
Preprint. Discussion started: 16 June 2026

Table 3. Statistical analysis of simulated significant wave height extracted along satellite tracks and at the wave buoy stations in terms of CRMSE, BIAS, CC and Slope. Statistics are reported as average values over the different Mediterranean sub-basins.

Sub-basin	Satellite				In-situ			
	CRMSE [m]	BIAS [m]	CC [/]	SLOPE [/]	CRMSE [m]	BIAS [m]	CC [/]	SLOPE [/]
Western	0.32	0.07	0.94	0.99	0.22	0.07	0.92	1.07
Tyrrhenian	0.29	0.08	0.92	1.03	0.22	0.04	0.94	1.05
Adriatic	0.32	0.03	0.87	1.07	0.18	0.01	0.87	0.93
Ionian-Meridional	0.27	0.03	0.93	0.94	0.24	0.06	0.92	1.03
Levantine-Aegean	0.26	0.03	0.91	0.93	-	-	-	-

3.2 Spatial and temporal distribution, influence area and duration of cyclones

The relative frequency of Mediterranean cyclones occurrence, defined as the number of tracks having a point within a radius of 50 km, regardless their phase of development, divided by the total number of tracks, is shown in Fig. 2a. The spatial distribution is not homogeneous and highlights some regions with higher frequency. The most intense cyclone activity is shown in the West MB, with the Ligurian Sea accounting for the highest density with a peak value of more than 6%: this area is known to be the most cyclogenetic one, cf. Trigo et al. (2002). We can observe a high cyclone occurrence also in the Tyrrhenian basin, especially in the area close to the Italian peninsula coast where spatial frequencies are in the range (3-6%), followed by the Northern African region (5%), close to the Atlas Mountain and the Lybian coast and finally the Cyprus area (spatial frequency larger than 3%). The Adriatic basin shows moderate cyclone frequency in its central part (>4%) while we remark that the northern part is characterized by very low cyclone occurrence.

Figure 2b shows the temporal frequency of cyclone influence area with respect to the period 1994-2020. It is computed by dividing the number of time that a grid point fall within any cyclone influence area by the total hindcast duration in hours. The figure highlights that the West-Meridional basin is the most influenced region by cyclones. The frequency decreases from this area following a concentric pattern toward the peripheral regions of the Mediterranean. The coasts of West, East and North Mediterranean are less influenced by cyclones, compared to the open sea areas. On the other hand, the coasts of the central Mediterranean such as Libya, Algeria, Sicily and south of Italy as well as West Greece display moderate frequency.

The mean cyclone influence areas (MCIA), expressed in terms of the fraction of the Mediterranean Sea surface influenced by the event, is shown in Fig. 3a. The median of the mean cyclone influence area corresponds to the 41% of the Mediterranean surface, while the extreme MCIA are larger than the 73% of the Mediterranean surface. We observe that no cyclones have a MCIA covering more than the 80% of the Mediterranean Sea. Figure 3b shows the relative frequency of MCIA that behaves like a bimodal distribution, with the two peaks at around 8% and 48%.

https://doi.org/10.5194/egusphere-2026-2774
Preprint. Discussion started: 16 June 2026

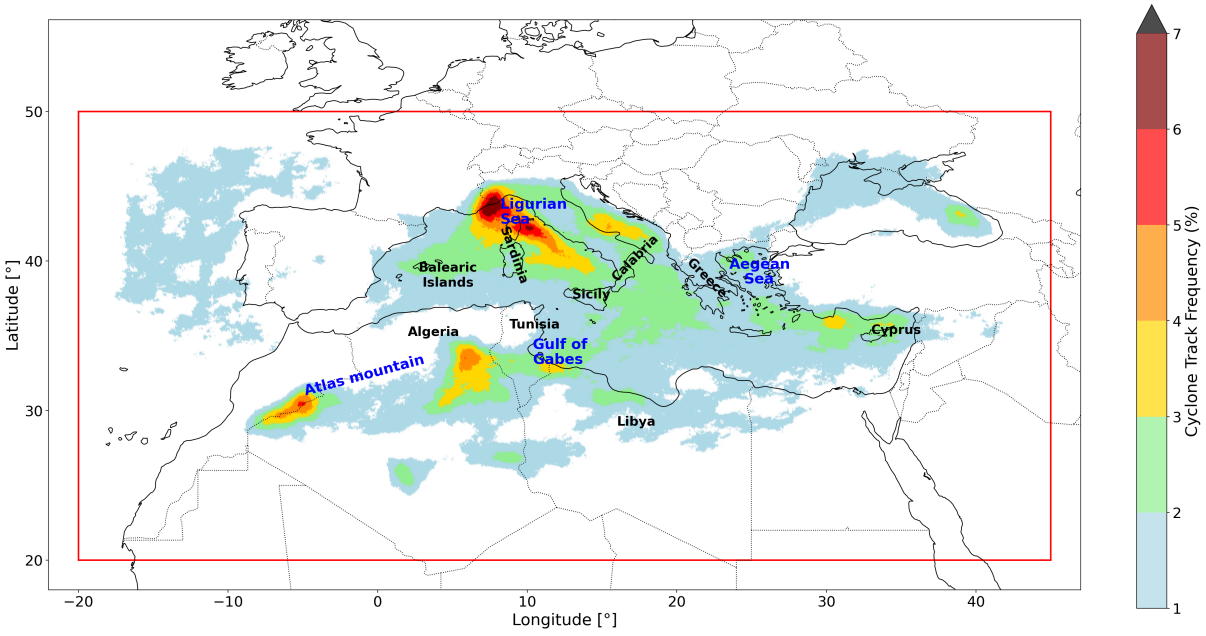

(a)

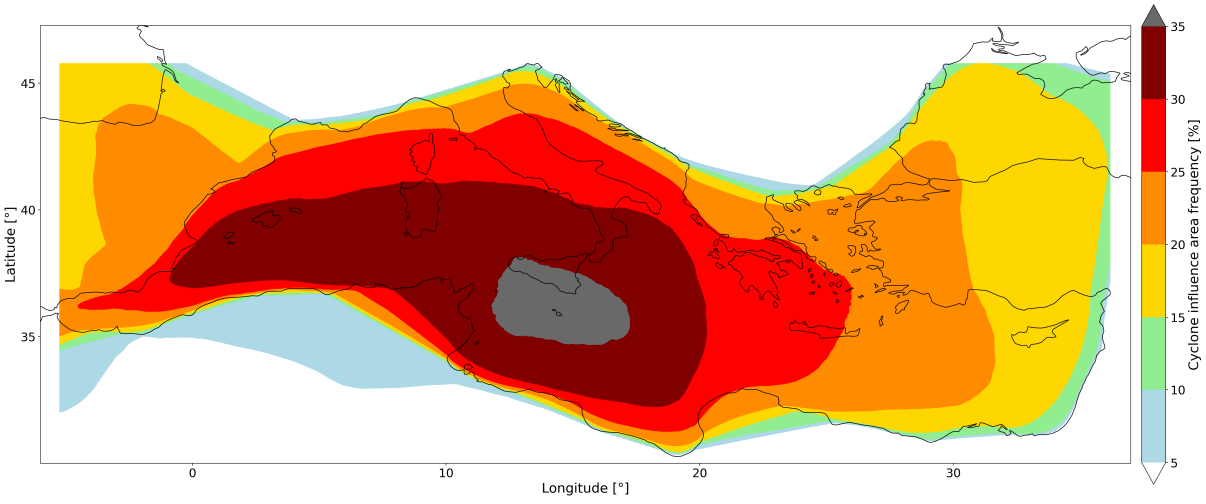

(b)

Figure 2. (a) Relative frequency of Mediterranean cyclones over the 1994– 2020 period, defined as the percentage of cyclones having a track point within a radius of 50 km. The red box indicates the area where cyclones are detected by Flaounas et al. (2023). **(b)** Relative occurrencies of cyclones influence areas over the 1994–2020 period, defined as the percentage of time during which a point is touched by any cyclone influence area.

https://doi.org/10.5194/egusphere-2026-2774
Preprint. Discussion started: 16 June 2026

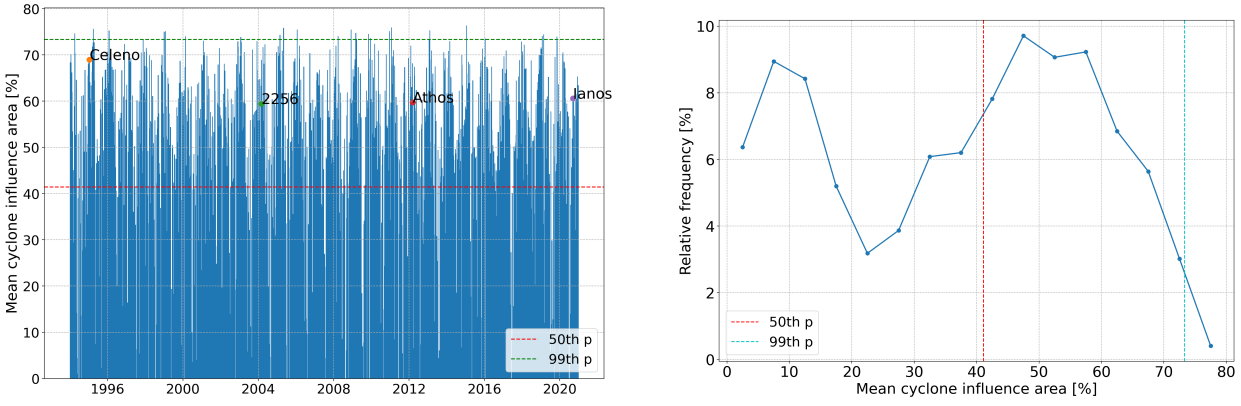

(a) (b)

Figure 3. (a) Time evolution of MCIA and corresponding percentiles. Names indicate cyclones for the selected case studies. **(b)** Relative frequency distribution of MCIA and corresponding percentiles.

330 The mean duration of the 2483 cyclones is equal to 69 hours (almost 3 days) while the maximum duration is 236 hours (about 10 days) (Fig. 4a). The total duration of cyclones represents the 58% of the time coverage of the investigated period (1994-2020), regardless the cyclone influence area (overlapping hours between different cyclones track points are excluded). The 50% of cyclones have a duration equal or less than about 2.5 days while extreme values of cyclones duration are larger than about 7 days (Fig. 4a). The distribution of the duration is Lognormal-like, skewed towards higher values, as it is shown in Fig. 4b.

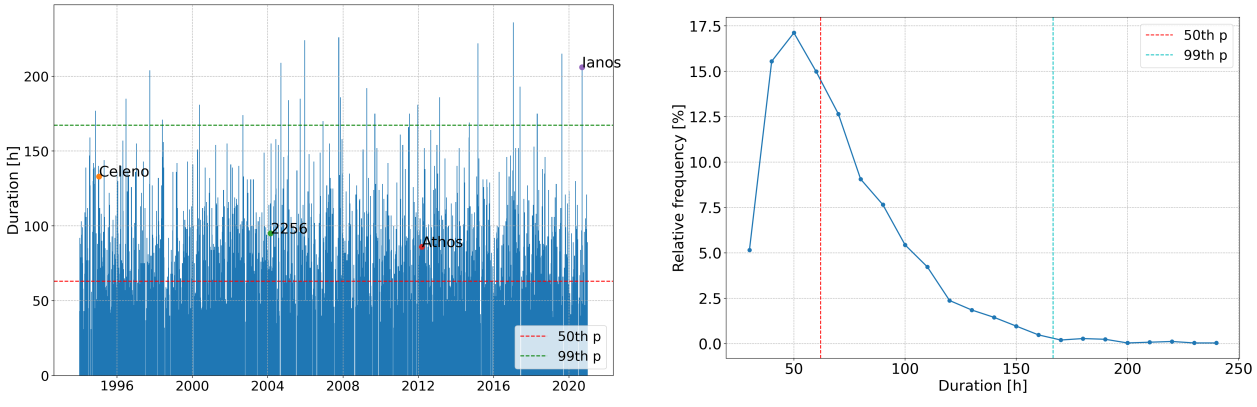

(a) (b)

Figure 4. (a) Time evolution of duration and corresponding percentiles. Names indicate cyclones for the selected case studies. **(b)** Relative frequency of cyclones duration and corresponding percentiles.

335

https://doi.org/10.5194/egusphere-2026-2774
Preprint. Discussion started: 16 June 2026

3.3 Storm surges and significant wave heights

In this section we consider two of the physical variables derived from the governing equations: the simulated storm surge and the simulated significant wave heights. We analyse their maximum values obtained along the cyclone duration and on the cyclone influence area and we study the link between the extreme conditions, given by the hindcast, and the subset of cyclones. The maximum value of max(S) is 1.29 m (Fig. 5a), while the mean is 0.32 m with a standard deviation of 0.17 m. The distribution of max(S) (Fig. 5b) is mildly asymmetric with positive skewness, as the mean is slightly larger than the median. Most cyclones have values of max(S) up to 0.5 m and the distribution is consistent with a Gamma-like shape. Figure 5c shows the spatial distribution of the 99^{th} percentiles for max(S) associated to cyclones in the Mediterranean basin. The Northern Adriatic basin shows the highest values of the 99^{th} percentile of max(S) which exceed 0.6m in the northernmost part. Other regions in the MB characterized by high values of max(S) are the Gulf of Gabès and the Western basin (the area between Sardinia and Balearic Islands) with values larger than 0.4 m. Most of the Thyrrenian basin shows extrem values of max(S) larger than 0.3 m, as well as most of the Ionian-Meridional basin. Compared to the rest of the MB, the Levantine-Aegean basin exhibits the lowest extreme values of max(S).

Values of max(H_s) associated to cyclones vary between [0.75, 11.23] m (Fig. 6a), the mean is equal to 4.33 m and the standard deviation is 1.62 m. As for max(S), the distribution of max(H_s) is a Gamma-like distribution, with a positive skewness (Fig. 6b). The spatial distribution of the 99^{th} percentile of max(H_s) associated to cyclones shown in Fig. 6c reveals significant differences compared to the one of max(S) (Fig. 5c). In particular, the Northern Adriatic is not marked out by high extreme values of maximum significant waves while is the case for the storm surge. The same difference is observed in the Gulf of Gabès and even slightly in the Tyrrhenian sea. On the other hand, the area between Sardinia and Balearic Islands concentrates highest values of the 99^{th} percentile of max(H_s).

We now observe the spatial distribution of the 99^{th} percentile for the storm surge and the significant wave height in the MB, computed over the whole simulation period 1994-2020 (Fig. 7a and 8a). As expected these maps display patterns similar to those associated with cyclones (Fig. 5c and 6c), although with weaker values because calm periods are included in addition to cyclones. The 99^{th} percentiles of Fig 7a and 8a correspond to values that are exceeded by only 1% of the entire hindcast. Fig. 7b and 8b illustrate the fraction of the upper 1% that is associated to cyclones in terms of storm surges and significant wave height corrispectively.

For storm surges, the west Mediterranean is the region where most of the extreme values are associated to cyclones. In particular, the large part of the Spanish Mediterranean coast is characterized by a strong link between extreme values of storm surge and cyclones (the percentage is larger than 60%). On the contrary in the Adriatic Sea, cyclones are driving less than 50% of the extreme values except along most of the Italian coast where percentage exceeds the 50%. The Ligurian Sea, the Aegean Sea and the Levantine basin, presents low percentages (between 30 and 50%) of extreme storm surge associated to cyclones. For the significant wave height, results show larger percentages of extreme values associated to cyclones with values up to 80%. The east coast of Sicily and the south coast of Calabria, the southern region of the Mediterranean Sea, the north-west

https://doi.org/10.5194/egusphere-2026-2774
Preprint. Discussion started: 16 June 2026

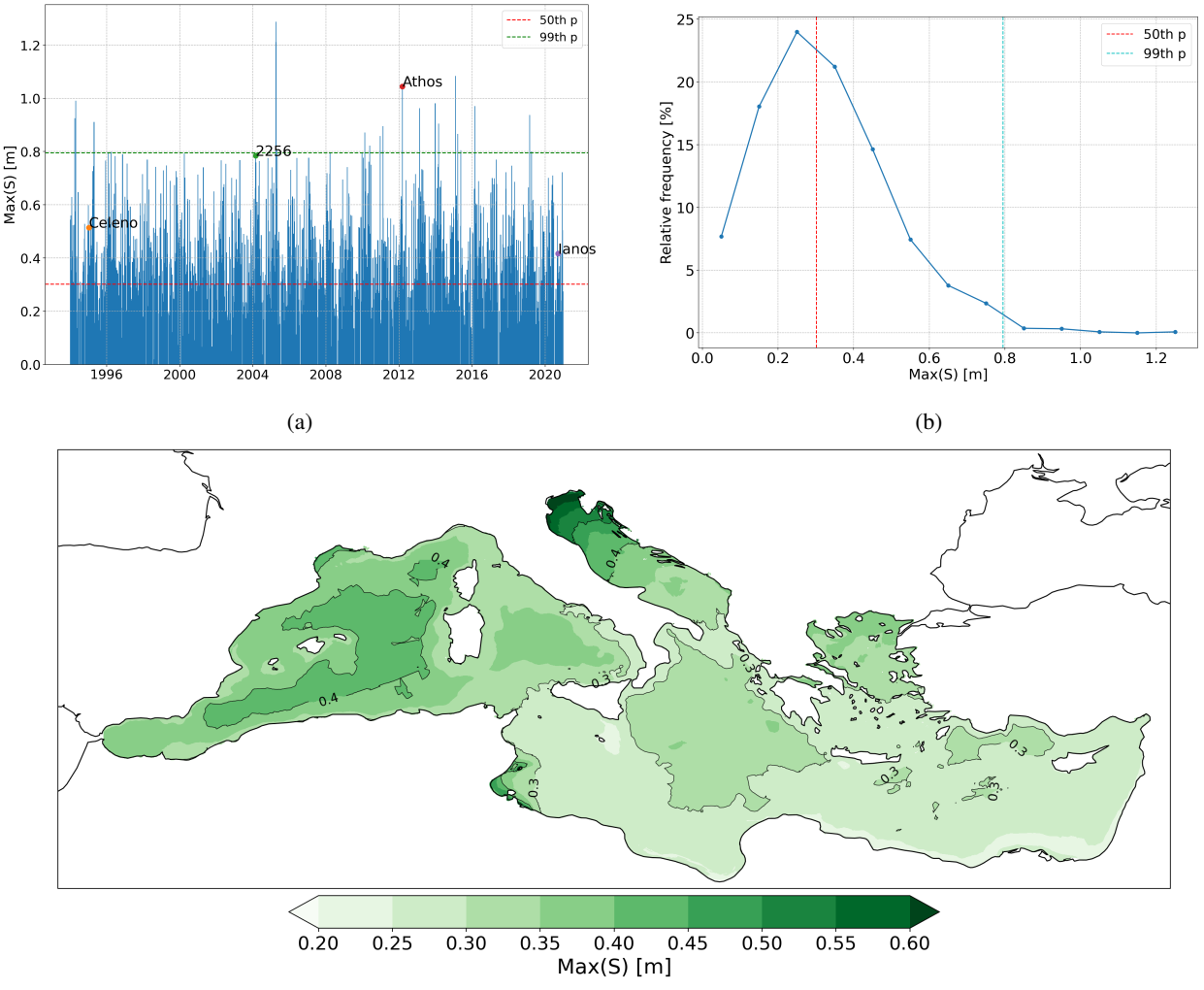

Figure 5. Time evolution of the cyclones maximum storm surge and corresponding percentiles (**a**). Names indicate cyclones for the selected case studies. Relative frequency of cyclones maximum storm surge and corresponding percentiles (**b**). Spatial distribution of 99^{th} percentile of the maximum storm surge (**c**).

370 part of the Aegean Sea and the western part of the Adriatic Sea are regions where the extreme values are largely represented by cyclones with more than 70% of data associated to cyclones. Finally, we remark that lower values of percentage (less than 50%) are shown in the Ligurian Sea, in the Tyrrhenian Sea (along the coast of the Italian peninsula) and in the Western basin, close to the Gibraltar strait.

https://doi.org/10.5194/egusphere-2026-2774
Preprint. Discussion started: 16 June 2026

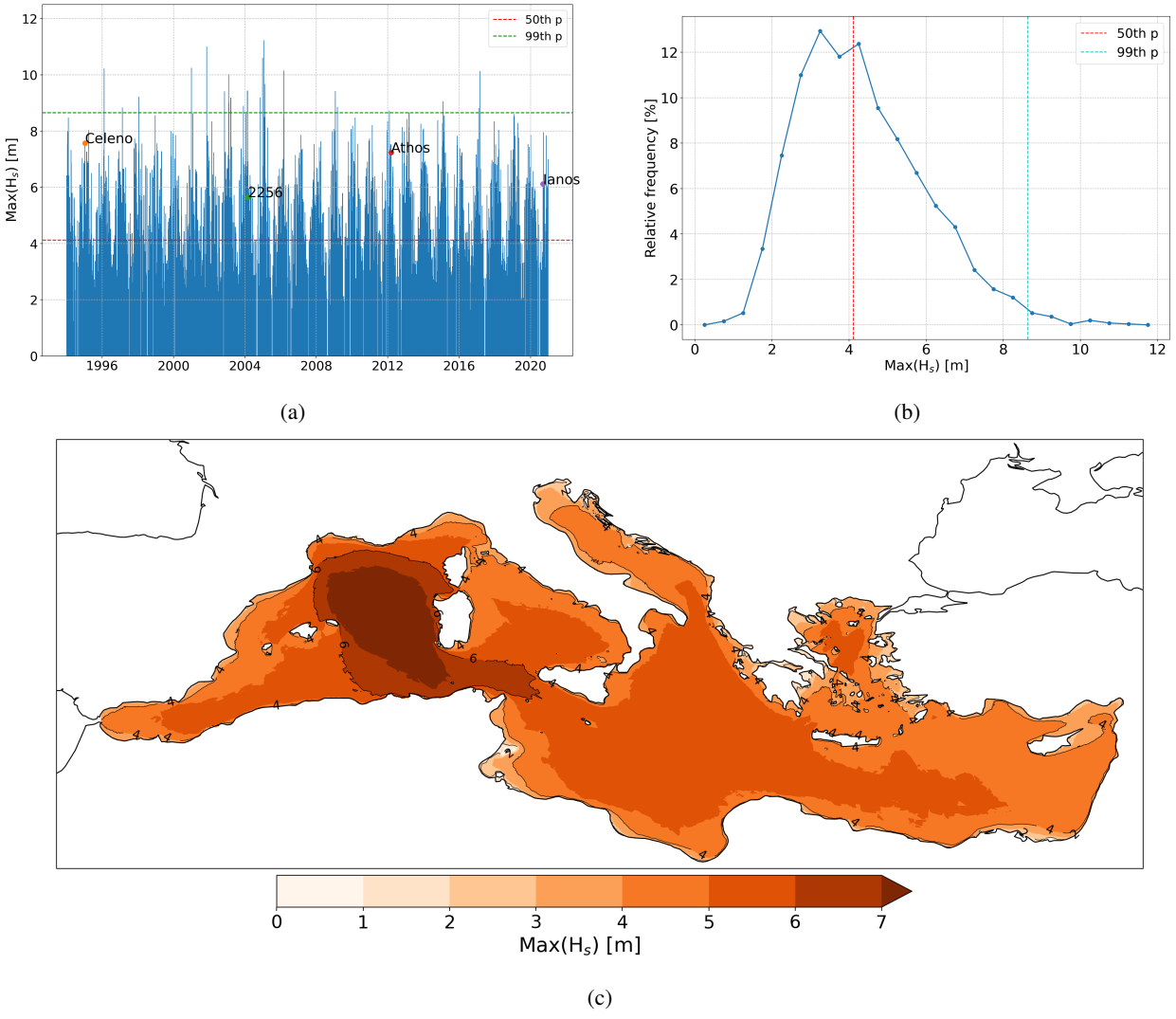

Figure 6. Time evolution of the cyclones maximum significative wave height and corresponding percentiles (**a**). Names indicate cyclones for the selected case studies. Relative frequency of cyclones maximum significative wave height and corresponding percentiles (**b**). Spatial distribution of 99^{th} percentile of the maximum significant wave height (**c**).

3.4 Cyclone magnitude indices

In this section we show results concerning the indices derived from waves and hydrodynamics: the total storm wave energy and the storm erosion potential index. Compared to the maximum of storm surge and of significant wave height, the total storm wave energy and the storm erosion potential index give a complementary information on cyclones hazard as they are obtained through a space-time integration of simulated wave power (for TSWE) and simulated sea levels and storm surge (for SEPI).

https://doi.org/10.5194/egusphere-2026-2774
Preprint. Discussion started: 16 June 2026

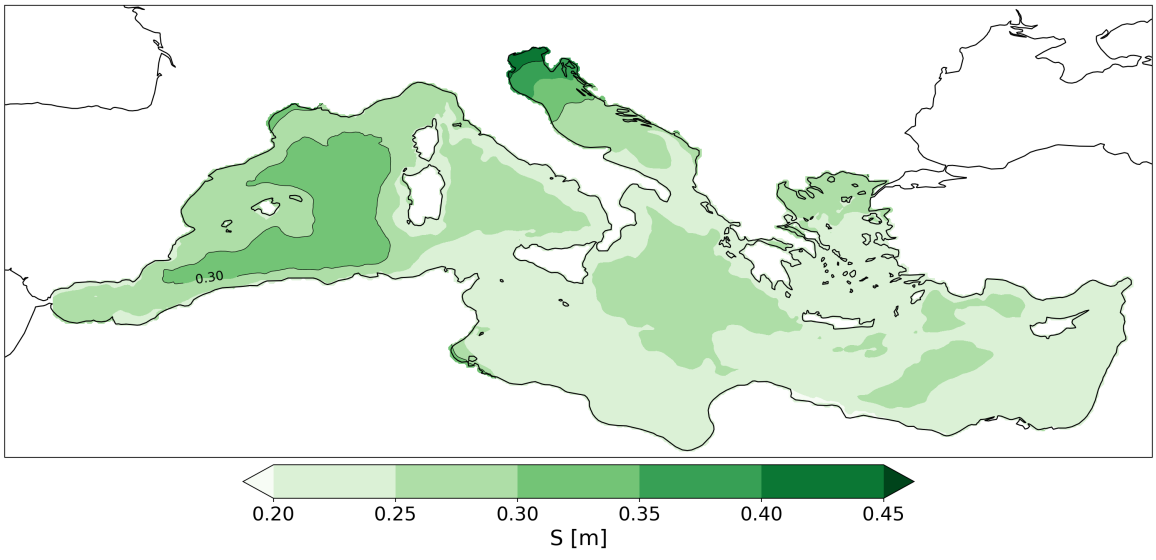

(a)

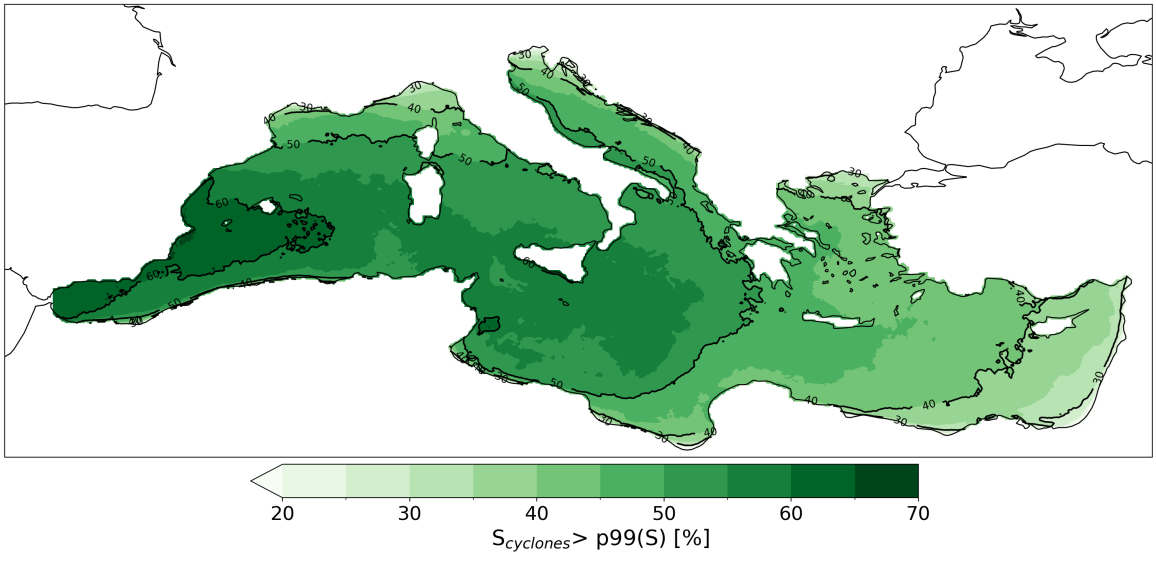

(b)

Figure 7. Spatial distribution of 99^{th} percentile of storm surge (**a**) and fraction of extreme events (S>99^{th} percentile) associated to cyclones (**b**).

Total storm wave energy

Figure 9a shows the evolution of the TSWE for each cyclone of the dataset with the corresponding 50^{th} and 99thth percentile

https://doi.org/10.5194/egusphere-2026-2774
Preprint. Discussion started: 16 June 2026

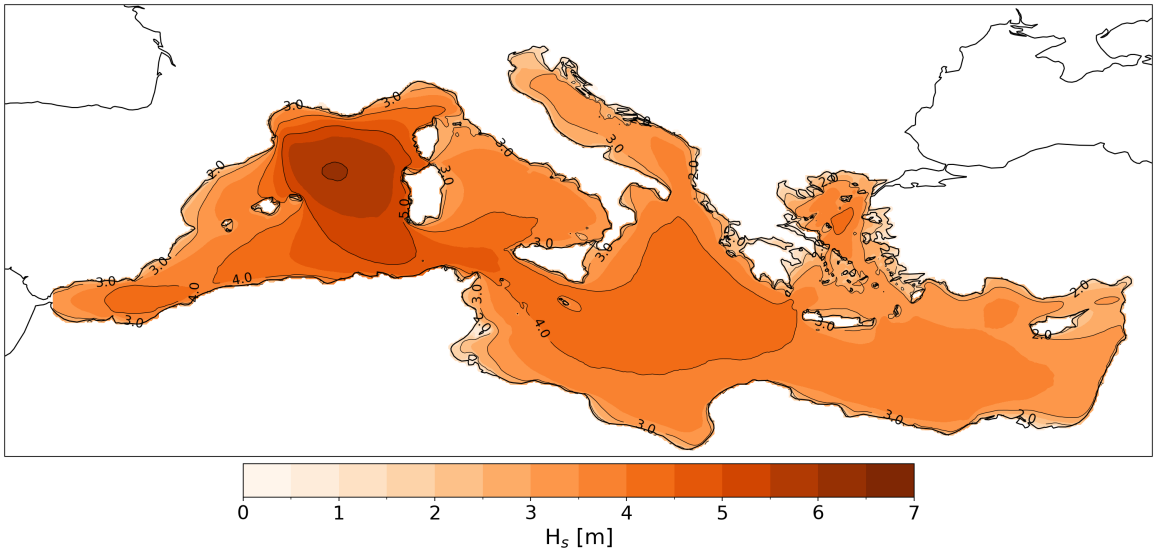

(a)

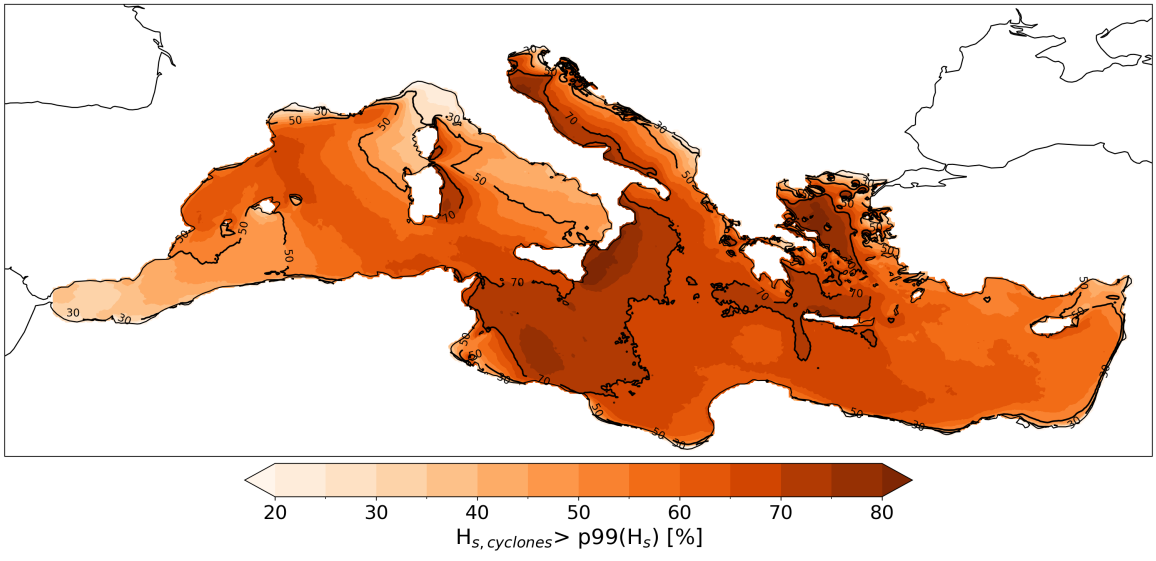

(b)

Figure 8. Spatial distribution of 99^{th} percentile of significant wave height (**a**) and fraction of extreme events (H_s>99^{th} percentile) associated to cyclones (**b**).

values. The average value is 5.10×10^5 $\mathrm{Wh/m}$ with a standard deviation of 5.53×10^5 $\mathrm{Wh/m}$. The distribution of TSWE is Lognormal-like, with a long tail to the right (Fig. 9b).

https://doi.org/10.5194/egusphere-2026-2774
Preprint. Discussion started: 16 June 2026

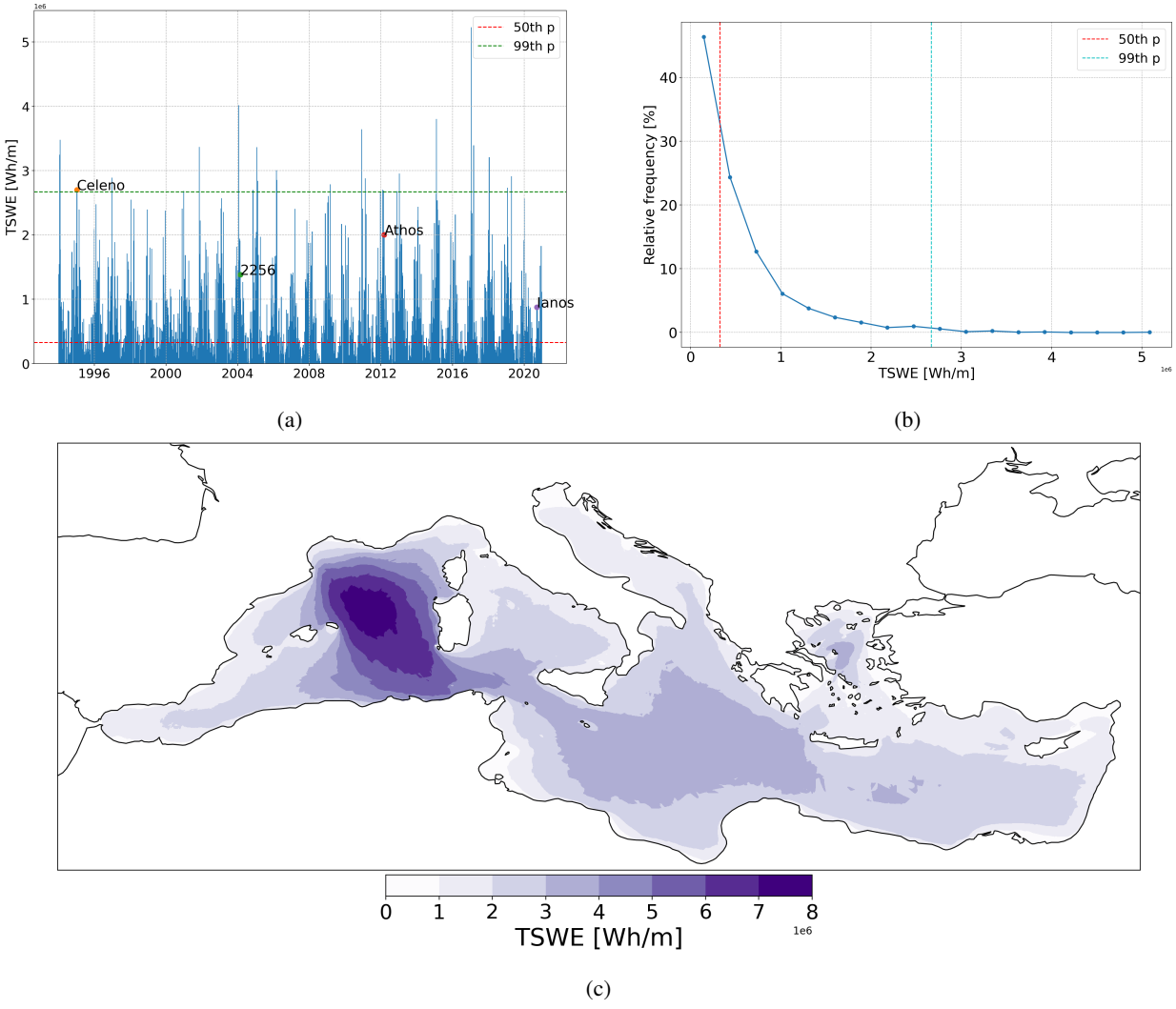

Figure 9. Time evolution of the cyclones TSWE and corresponding percetiles (**a**). Names indicate cyclones for the selected case studies. Relative frequency of cyclones TSWE and corresponding percentiles (**b**). Spatial distribution of the 99^{th} percentile of cyclones TSWE (**c**).

As the index is based on variables related to waves, results agree with the maps showing the spatial distribution of the 99^{th} percentile for the maximum significant wave heights (Fig. 6c). Indeed, the Western Mediterranean Sea is the region with higher values of the 99^{th} percentile of TSWE, while moderate values are also observed in the southern part of Mediterranean Sea. Regions with lower values of 99^{th} percentile are the Adriatic basin, the east and west Mediterranean (i.e. Alboran Sea). Results agree with those obtained in the Western Mediterranean Sea by Amarouche et al. (2022).

Storm erosion potential index

SEPI values for each cyclone of the dataset and their percentiles are shown in Fig. 10a. This index, based on sea level and storm

https://doi.org/10.5194/egusphere-2026-2774
Preprint. Discussion started: 16 June 2026

surge, as a maximum value of 2.4 $\mathrm{m^2\,h}$. The average value is equal to 0.025 $\mathrm{m^2\,h}$, with a standard deviation of 0.13 $\mathrm{m^2\,h}$. The distribution of SEPI, shown in Fig. 10b, stress that most of the cyclones are weak according to this parameter while a few cyclones are very intense, contributing to a long upper tail. The spatial distribution of the 99^{th} percentile is shown in Fig. 10c where we observe that areas with higher values of SEPI are the Western Mediterranean and the Northern Adriatic Sea. Since SEPI is partially based on simulated storm surge, we compare the map of the 99^{th} percentile of max(S) (Fig. 5c) with Fig. 10c. Similar patterns between the two variables are observed, except in the Gulf of Gabès and the Northern Aegean Sea.

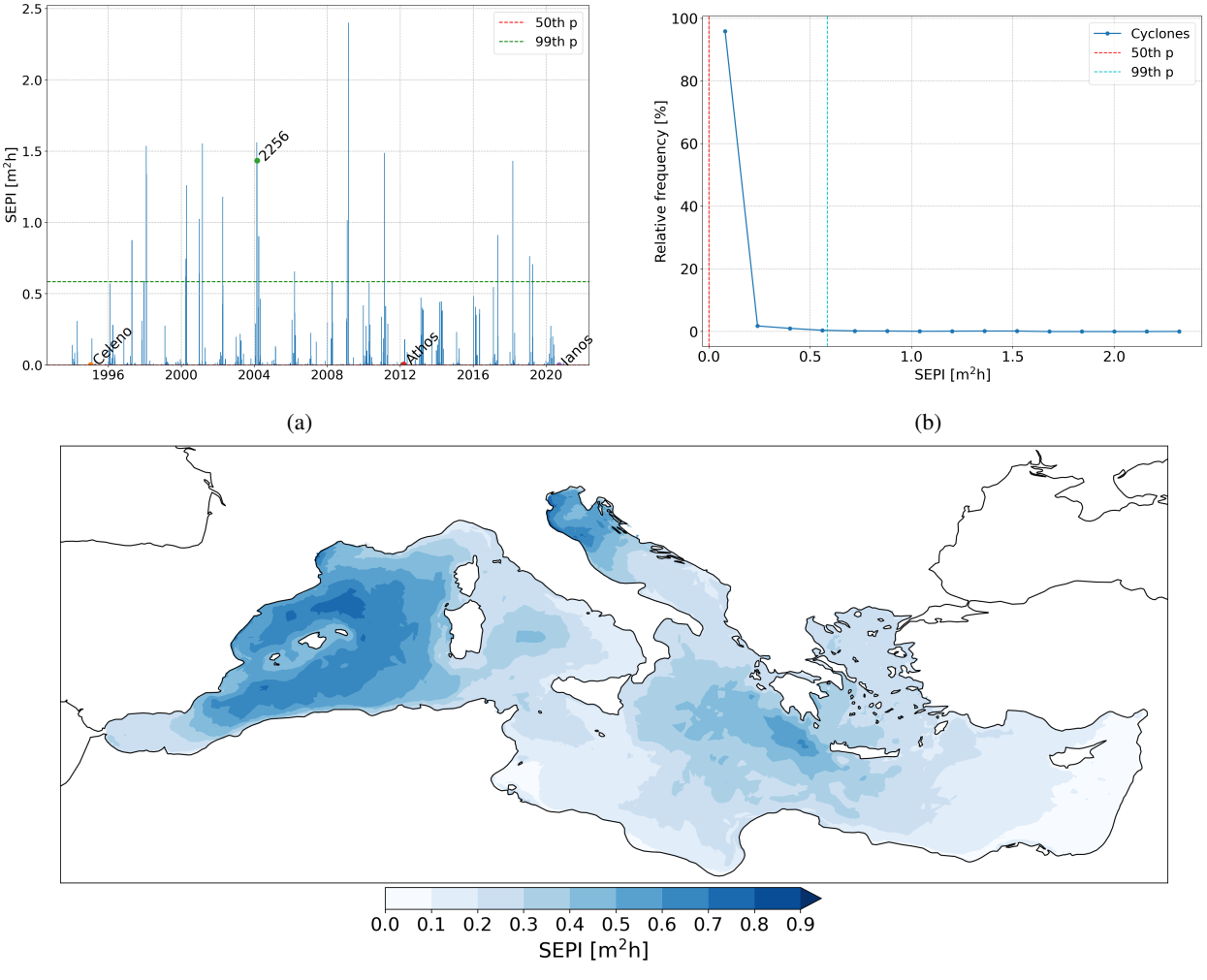

Figure 10. Time evolution of the cyclones SEPI and corresponding percentiles (**a**). Names indicate cyclones for the selected case studies. Relative frequency of cyclones SEPI and corresponding percentiles (**b**). Spatial distribution of the 99^{th} percentile of cyclones SEPI (**c**).

https://doi.org/10.5194/egusphere-2026-2774
Preprint. Discussion started: 16 June 2026

3.5 Case studies

The marine and coastal hazard is investigated with a more detalied analysis for four cyclones belonging to the dataset. We choose four intense events characterized by extreme values according to at least one hazard parameter. Two of these events, Celeno and Ianos, correspond to well known intense cyclones which are classified as medicanes (see Miglietta et al. (2025) for a detailed medicane definition), already studied in the literature. Events are listed in Table 4 where hazard parameters for every cyclone are also indicated. Cyclone 2256 affects mainly the Western, the Tyrrhenian and Adriatic basin, while the Ionian-Meridional basin is affected by cyclone Celeno, Athos and Ianos.

Table 4. List of selected case study and corresponding values of hazard parameters. ID corresponds to the index used to identify cyclone in TRACKS CL5.

Name	ID	Start date	Duration [h]	MCIA [%]	Max(S) [m]	Max(H_s) [m]	SEPI [m^2 h]	TSWE [Wh m^{-1}]
Celeno	1410	1995/01/13	133	69	0.51	7.57	1×10^{-4}	2.7×10^{6}
/	2256	2004/02/26	95	59	0.78	5.64	1.43	1.38×10^{6}
Athos	3006	2012/03/08	86	60	1.04	7.24	4×10^{-3}	2×10^{6}
Ianos	3777	2020/09/12	206	61	0.42	6.11	4×10^{-5}	8.74×10^{5}

Cyclone Celeno (Avolio et al., 2024) has a duration that exceeds 5 days but is smaller than the threshold of the 99^{th} percentile (Fig. 4a). It influenced a large portion of the MB (MCIA = 69%) and according to the TSWE it can be classified as an extreme event. Cyclone Celeno is characterized by high values of significant wave height over a large zone in the Mediterranean. Indeed, during this event, there are several spots inside the cyclone influence area with wind velocity larger than 18 $\mathrm{m\,s^{-1}}$ generating severe sea state. High, spatially widespread, persistent values of significant wave height combined with a long cyclone duration, result in a highly energetic cyclone, as reflected by the large TSWE values (Fig. 11). Although meteorological conditions strongly determinate such a severe sea state, a comparable response is not observed in the storm surge component. We observe an inverse barometer effect in the area surrounding the cyclone track and high storm surge values in the Gulf of Gabès, favored by the exceptionally wide, gently sloping, and shallow continental shelf. Nevertheless, cyclone Celeno cannot be classified as extreme event in terms of storm surge magnitude.

Cyclone Athos ranks among the most intense events in our dataset in terms of maximum storm surge, which is observed in the Gulf of Gabès. This cyclone has a short lifetime, about 3.5 days, compared to the other selected cyclones (Fig. 4a) and the value of MCIA lies in the region between the median and the 99^{th} percentile, as shown in Fig. 3a. The system develops over north Africa and enters the Mediterranean Sea, approaching the Tunisian coast on the evening of 9 March. It then remains in the Meridional basin where it dissipates. Athos is characterized by moderate to strong wind speed (exceeding 18 $\mathrm{m\,s{-}1}$) along the marine side of its track. The intense winds over the Gulf of Gabès, together with the region's particularly gentle and shallow continental shelf, are also responsible of extreme storm surge conditions. Storm surge levels exceed 1 m several times throughout the cyclone's lifetime and nearly the entire Gulf of Gabès is associated with extreme surge values as shown

https://doi.org/10.5194/egusphere-2026-2774
Preprint. Discussion started: 16 June 2026

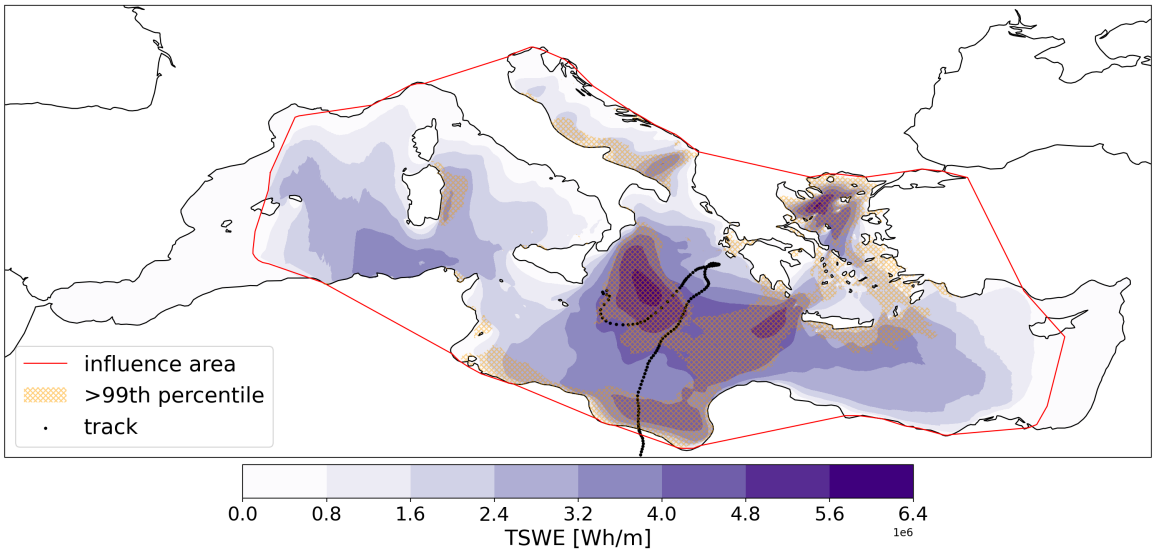

Figure 11. Spatial distribution of TSWE for cyclone Celeno.

in Fig. 12. Though high values of storm surge, the associated SEPI is low likely because the condition on water levels is not satisfied (i.e. condition $Z(t) \geq \overline{MHHW}$). The significant wave height reaches and locally exceeds 7 m (on 9 March), while values predominantly range between 4 and 6 m during the remaining time.

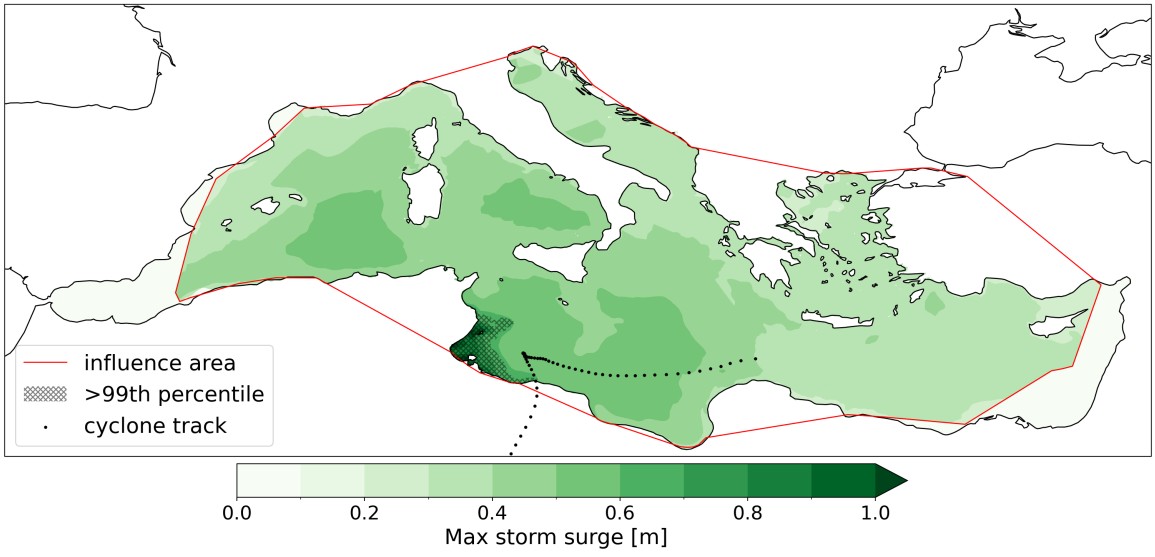

Figure 12. Spatial distribution of maximum storm surge for cyclone Athos.

https://doi.org/10.5194/egusphere-2026-2774
Preprint. Discussion started: 16 June 2026

Among the four cyclones, cyclone 2256 is the most intense cyclone according to SEPI. This event is also characterized by a significative maximum storm surge (5a) while other hazard parameters are not extreme. This cyclone develops over the Ligurian Sea and moves towards the Italian peninsula with a south-east direction. Intense winds occur along and around the cyclone track, generating significant wave heights with maxima larger than 5 m in the Thyrrenian basin. During cyclone passage, high values of storm surge are observed in the Thyrrenian and Adriatic basin where the value of 0.7 m is reached. This factor, combined with sea levels frequently exceeding Mean Higher High Water (MHHW), results in extreme SEPI values, as shown in Fig. 13.

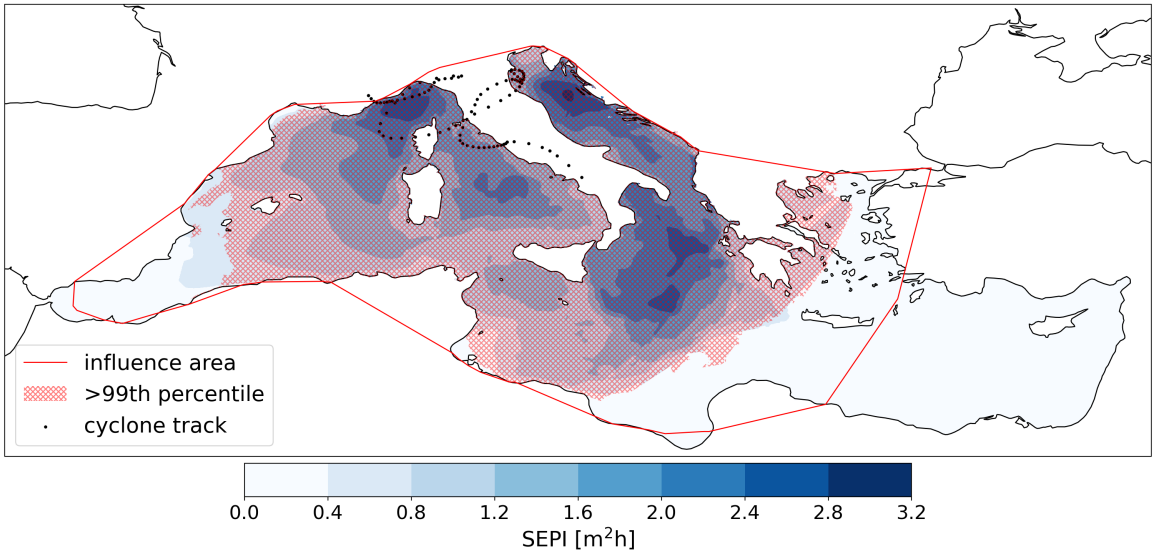

Figure 13. Spatial distribution of SEPI for cyclone 2256.

Cyclone Ianos (Lagouvardos et al., 2022; Ferrarin et al., 2023; Scardino et al., 2025; Babagolimatikolaei, 2026), is one of the longest-lasting cyclones in our dataset with a lifespan exceeding eight days (Fig. 4a). The cylogenesis phase occurs in Lybia while the mature phase develops in the Ionian-Meridional basin, near the coasts of Calabria and Greece. During its mature stage, Ianos exhibits strong and sustained surface winds (higher than 20 $\mathrm{m\,s^{-1}}$) around the cyclone center, generating severe marine conditions. Significant wave heights reach up to 6 m along the Greek coast, exceeding the 99^{th} percentile within a limited area (Fig. 14a). Storm surge is also significant in the area surrounding the cyclone track during the mature phase, altough values remain below the 99^{th} percentile threshold (Fig. 14b). Both extreme wave heights and elevated storm surge levels are confined to a relatively small area along the Greek coast compared to the overall spatial extent of the cyclone's influence. Therefore, from a meto-marine point of view, medicane Ianos can be characterized as an intense but localized event. For this reason, marine hazard indices do not identify it as one of the most extreme events of our dataset (Fig. 5a, 6a, 9a,10a), despite its long duration. All these cyclones are highly intense, although their intensity arises from different characteristics.

https://doi.org/10.5194/egusphere-2026-2774
Preprint. Discussion started: 16 June 2026

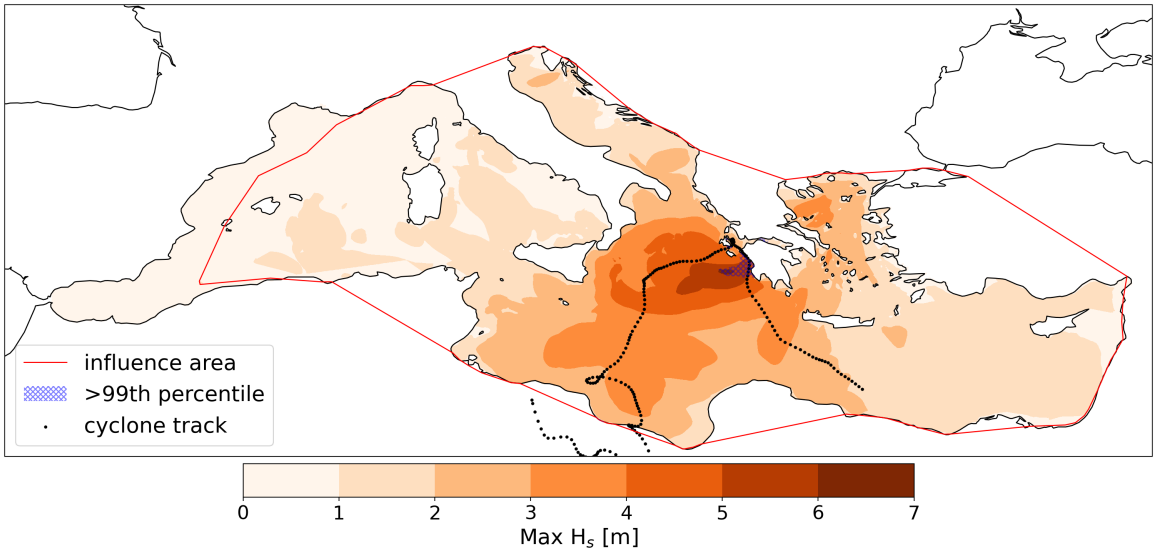

(a)

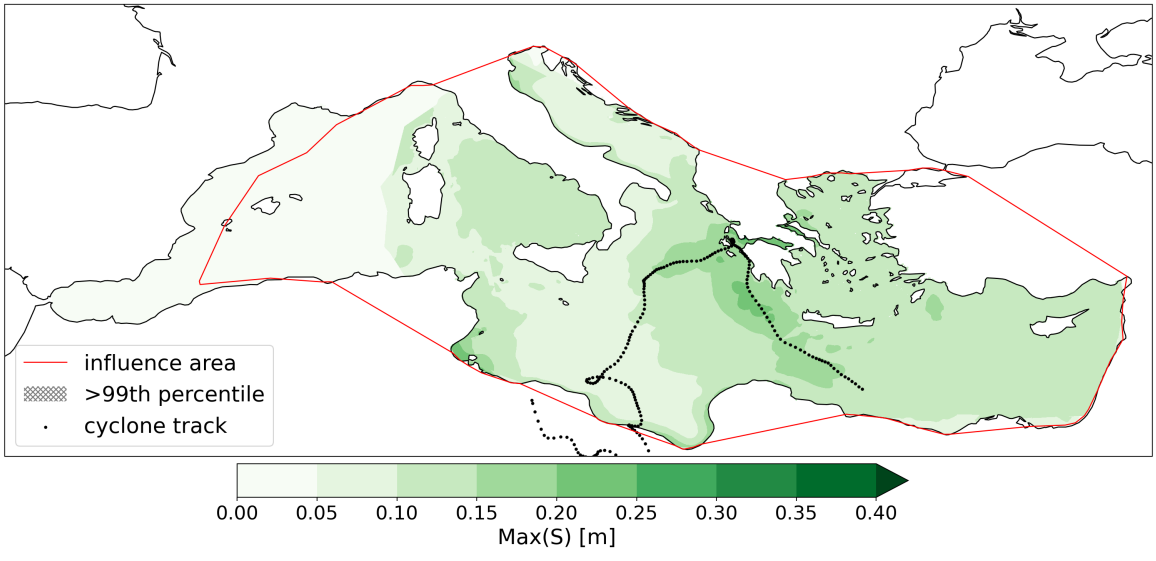

(b)

Figure 14. Spatial distribution of some hazard parameters for cyclone Ianos: maximum significant wave height (**a**) and maximum storm surge (**b**).

This demonstrates that is necessary to consider different parameters to characterize the hazard since each parameter provides different measures of intensity and the latter are not necessarily correlated (e.g. classification differs depending on the parameter

https://doi.org/10.5194/egusphere-2026-2774
Preprint. Discussion started: 16 June 2026

chosen).

4 Discussion

In literature there are several studies that analyse the marine and coastal hazard of one or more specific events (Scicchitano et al., 2021; Mattei et al., 2021; Ferrarin et al., 2023; Flaounas et al., 2025), while in this study we aim to characterize the relative role of cyclones in determining marine hazardous conditions.

We find similar works (Amarouche et al., 2022; Martzikos et al., 2021) where only some of the hazard parameters that we use are analyzed in a limited region of the MB or for a series of buoys. In Amarouche et al. (2022) the analysis of wave storm events is focused on the Western Mediterranean basin and the spatial distribution of maximum significant wave height and TSWE during wave storm events (identified through a threshold on the significant wave height) recorded over the last four decades (1980-2020) has similar patterns to those that we obtain (Fig. 6c and 9c). Our study completes the analysis by considering the whole MB showing that the Western basin, in particular the area between Sardinia and Balearic islands remains the portion of the Mediterranean Sea with highest values of the 99^{th} percentile of maximum significant wave height induced by cyclones. Our results of the TSWE show that the Ionian and Southern MB are characterized by moderate values of cyclones energy (according to the 99^{th} percentile), even if they are lower than those in the Western basin.

In Martzikos et al. (2021), 4008 coastal storms are analysed, corresponding to 41-127 Mediterranean storm events per year, which is in agreement with our study that considers 92 cyclones per year in average. Martzikos et al. (2021) perform a coastal storm analysis by studying the parameters which define a coastal storm and their properties, such as the wave height, the wave period, the duration, the calm period, and the storm energy. Results of this study describe cyclone intensity in some specific buoys location, according to the temporal availability of the measures. Our analysis completes the characterization of cyclones including parameters related to sea levels and considering the whole MB, for a continuous period of 27 years, thanks to the numerical hindcast of sea levels and wind-waves.

Results about the maximum storm surge induced by cyclones (Fig. 5c) confirm that coastal regions with wide continental shelves, gentile slope and shollow waters are among the most affected one, like the Northern Adriatic Sea and the Gulf of Gabès. This can be extensively verified in other works like Marcos et al. (2009); Conte and Lionello (2014); Lionello et al. (2017); Boyes and Elliott (2019); Toomey et al. (2022a); Makris et al. (2023). The storm surge observed in the Western basin, a small portion of the Thyrrenian and of the Meridional basin is mainly related to the inverse barometer effect rather than wind which is the dominant factor only in shallow areas (Lionello et al., 2019; Conte and Lionello, 2013).

Results on the percentage of extreme data associated to cyclones (Fig. 7 and 8) shows that, in general, extreme waves are more frequently associated with well defined low-pressure systems than extreme storm surge and there is not spatial correlation between them. The spatial difference between the percentage associated to cyclones for waves and storm surge, is also linked to cyclones physics as these systems are characterized by a rotating wind field around a low pressure center, with strongest wind occurring in a ring rather than in the cyclone center. For this reason, under open sea conditions the location of maximum values

https://doi.org/10.5194/egusphere-2026-2774
Preprint. Discussion started: 16 June 2026

of storm surge and significant wave heights are not expected to be in the same position. In addition, the local morfology and the bathymetry play an important role modifying the sea levels and waves response approaching the coast. For all these reasons, the concurrence between extreme storm surges and high waves is not straightforward and is dependent on site conditions. The few percentage of extreme data associated to cyclones in some specific regions of the MB can also be explained by the presence of local and regional winds (e.g. mistral and bora), able to create extreme sea conditions without being necessarily associated to well-organized low pressure systems in the Mediterranean. In Marcos et al. (2019) authors investigate the relationship between extreme storm surges and waves along the world coastlines, showing that, for the Mediterranean coast, the dependence between extreme storm surge and waves is extremly variable according to the geographical location. Values of dependence strenght and of Kendall rank correlation coefficient show that there is not a strong dependence, except for a few points that are located in the north-Africa coast, in the Northern Adriatic basin and in the eastern coasts of Mediterranean.

Distributions of hazard parameters (Fig. 3b, 4b, 5b, 6b, 9b, 10b) show that TSWE and SEPI, compared to other parameters, have very different distributions with many very small values and few large values. A similar difference between dynamical measures and impact-relevant measures of cyclones intensity is observed in Cornér et al. (2025). The bimodal distribution of MCIA reveals two cyclones classes related to the track region: the first one characterized by smaller MCIA corresponds to cyclones whose track points are mainly outside of the MB, the second one characterized by larger MCIA corresponds to cyclones whose track points are inside the MB (Fig. S4 in the Supplement). This result is linked to the method chosen to compute the cyclone influence area, where only the sea surface is considered (wind field over the land is excluded).

The investigation of four selected case study shows that intense storms are not necessarily characterized by extreme values of every hazard parameter. Cyclones corresponding to the most extended duration as Ianos, are not particularly ones with maximum significant wave height or storm surge (and viceversa). Moreover, they do not correspond to cyclones with strong intensity according to TSWE and SEPI, although these indices account for cyclone duration. This underlines the importance of considering different hazard parameters when characterizing cyclones. Indeed, it is clear that peak parameters as max(H_s) and max(S) fournish an istantaneous snapshot of cyclone intensity while cumulated indices like TSWE and SEPI give an integrated overview that considers the intensity of single variables (e.g. significant wave height, wave period, sea levels and storm surge levels) combined with cyclone duration and cyclone spatial influence. Intense cyclones of our dataset are not necessarily well-known cyclones (i.e. damaging and impactful cyclones) since our statistical analysis is based on climatological values (e.g. 99th percentile) and on cyclone dataset where all the cyclone life stages (cyclogenesis/mature stage/cyclolysis) are considered, without discriminating between land, coastal and open sea areas. In addition, we limit this work to the hazard analysis: vulnerability and exposure of the areas affected by cyclones are not considered and they are key factors of impactful cyclones. Finally, impactful cyclones can be related to precipitations or compound events like wind gusts and precipitations, which are not considerd in this work.

Our study stresses that different cyclone classifications could be obtained according to the chosen hazard parameter. For this reason we investigate the relationship between the hazard parameters selected in this work performing a correlation analysis with two different methods. The first one is the Pearson's correlation coefficient (r) to measure the linear relationship between two variables (X,Y) corresponding to the ratio between the covariance of two random variables and their standard deviations.

https://doi.org/10.5194/egusphere-2026-2774
Preprint. Discussion started: 16 June 2026

The second method is the mutual information (MI), which is a measure of the amount of information one random variable contains about another (Cover and Thomas, 2006). It is the reduction in the uncertainty of one random variable due to the knowledge of the other and is used to quantify non-linear dependencies. The MI values which belong to the interval [0, inf] are converted into a correlation coefficient (ρ) with values between 0 and 1 by normalization, thanks to the Python package ennemi (Laarne et al., 2021, 2022). The normalization ensures that results are easily interpretable (0 means poor correlation while 1 means strong correlation) and comparable to the Pearson coefficient: in classical linear correlation, it matches the Pearson correlation coefficient, except for missing the sign (Laarne et al., 2022). Equal or similar values of r and ρ states that the variables are linearly correlated while higher values of ρ means that there is a non-linear relationship. The results for the Pearson coefficient and the MI coefficient are shown in Fig. 15. The Pearson correlation coefficients are statistically significant for all the variables combinations (p-values are lower than 0.05). We observe an high (r > 0.7) Pearson correlation coefficient between the wave-based magnitude index (TSWE) and the maximum significant wave heights, which can be expected due to the TSWE formulation (see Equation (9)). However, relationship is not perfectly linear, as cyclones with high values of max(H_s) can be characterized by either short or long cyclone lifetime (that means low or high values of TSWE), resulting in a large dispersion for high values of max(H_s). The mean cyclone influence area has low correlations with other variables, except with max(H_s) (r = 0.54). This moderate correlation can be partially explained by the fact that the MCIA is a rough proxy of the fetch. Low values of Pearson correlations are found for all other variable pairs. We compare now the Pearson coefficients with the MI correlation coefficients. The relationship between the wave-based magnitude index and the maximum significant wave height is strong even according to the MI correlation coefficient (ρ = 0.88). The MI correlation coefficient for the pair (max(S),SEPI) shows a stronger realtionship, which is not detected by the Pearson coefficient. Indeed the MI correlation coefficient is almost the double of the Pearson coefficient (r = 0.31 and ρ = 0.61), suggesting a dominant non-linear component in the relationship between these two variables. The thresholds used in the SEPI formulation (see Eq. (6)) and the influence of sea levels in the SEPI results are probably the key factors driving the non-linearity between max(S) and SEPI. All other variables show slightly increased MI coefficients compared to Pearson coefficients, however most of the values are lower than 0.5 indicating a weak relationship between them.

The use of a meteorological method for cyclone detection implies a correspondence between the event from both an atmospheric and a marine point of view. We do not expect that events detected through this approach are equal in number and temporal characteristics to events detected through a threshold method on hydrodynamic variables (e.g. significant wave height). However, we are confident that the potential error on cyclone duration (and on the start/end date of the event) is negligeable since the cyclone tracking and detection method considers cyclones from the cyclogenesis to the cyclolysis and significant marine effects are typically associated to the mature stage of cyclones when they reach the highest intensity. Another limitation of this study is the use of a specific cyclone dataset (TRACKS CL5). It is known that results in term of spatial frequency, cyclone duration and position are dependent on the tracking algorithm because of variables and thresholds use to identify cyclones. Consequently, even the results related to the ocean component suffer of this dependency. Finally, the method proposed to compute the influence area (so the hazard parameters inside it) presents some limits. Firstly, the influence area is dependent on the wind speed threshold. Secondly, it does not allow to distinguish between events that occur at the same time and in a

https://doi.org/10.5194/egusphere-2026-2774
Preprint. Discussion started: 16 June 2026

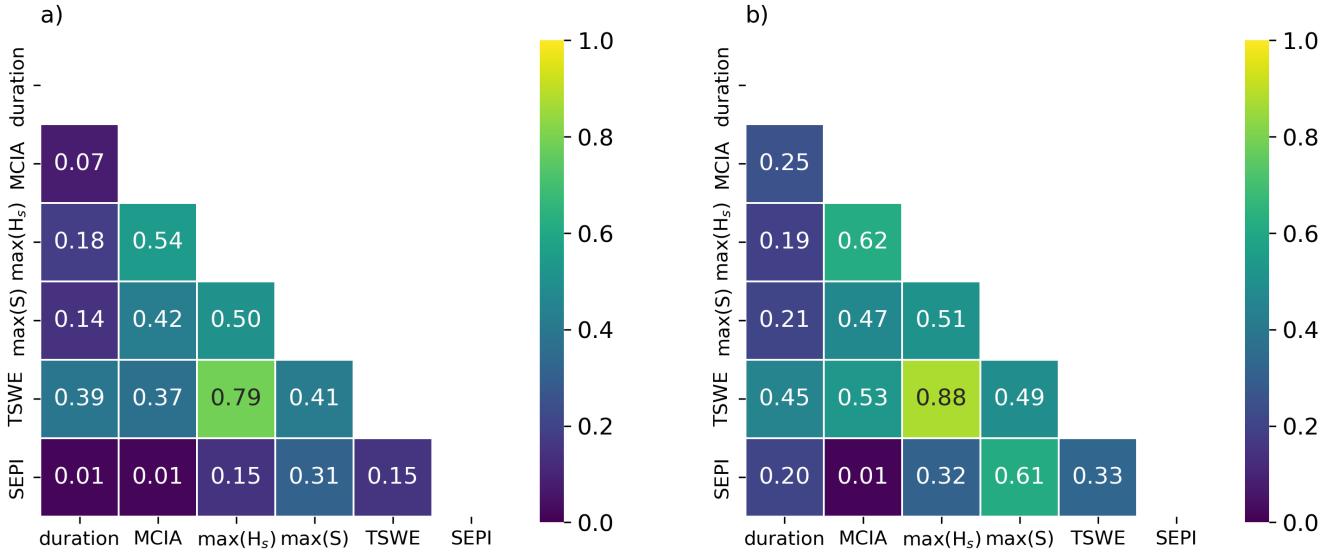

Figure 15. Pearson (**a**) and Mutual Information (**b**) correlation coefficients for the selected variables describing coastal and marine cyclone hazard.

relative small spatial area: they will share the same influence area. Despite these limitations, our study offers some new insights into cyclones hazard characteristics in the MB, highlighting importance of hazard parameters for a comprehensive description of cyclones.

5 Conclusions

We created a 27 years (1994-2020) hindcast of sea levels and wind waves for the Mediterranean Sea to analyze the marine and coastal hazard of Mediterranean cyclones. The ocean hindcast is obtained through a 2D tide-wave-surge model and the cyclone subset (2483 events) is derived using an atmospheric composite cyclone detection and tracking method. Cyclone tracks and duration, along with wind fields, are used to define the portion of the Mediterranean basin influenced by each cyclone. The ocean simulation results are then processed over the influence areas to evaluate four parameters for characterizing marine and coastal hazards: maximum storm surge, maximum significant wave height, the storm erosion power index, and total storm wave energy. In this way, we create a dataset of Mediterranean cyclones hazard parameters.

The analysis of the model results allows for the evaluation of the fraction of extreme marine conditions in the Mediterranean Sea associated with cyclones. In the Western Mediterranean and the Ionian-Meridional basin, between 50% and 75% of storm surge and wave extremes, respectively, are linked to cyclones (with percentages exceeding 75% in some sub-regions of these basins, in case of wave extremes). In the Levantine–Aegean basin, more than 50% of wave extremes (and over 75% in the northern Aegean Sea) are associated with cyclones, whereas for storm surge the proportion is lower than 50% in the same area.

https://doi.org/10.5194/egusphere-2026-2774
Preprint. Discussion started: 16 June 2026

The cyclone hazard depends strongly on the selected parameter, as it can vary depending on the metric considered. Consequently, the strongest cyclones in terms of maximum significant wave height differ from those identified based on maximum storm surge or another hazard parameter. Due to this variability, it is challenging to identify the most hazardous Mediterranean cyclones, as well as the areas most exposed to hazard when it is considered in a comprehensive sense (i.e., accounting for all parameters).

Data availability. Hazard parameters of each cyclone are provided as a Supplement in the form of ASCII file made up by 2483 rows and 9 columns. Each row corresponds to a single cyclone and the nine columns provide the following information:

- Cyclone track index (corresponding to the one given in TRACKS CL5).
- Start date of the event in the format yyyy-mm-dd::hh:mm:ss.
- End date of the event in the format yyyy-mm-dd::hh:mm:ss.
- Cyclone duration in [h].
- Mean cyclone influence area in [%] with respect to the Mediterranean basin.
- Maximum storm surge in [m].
- Maximum significant wave height in [m].
- Storm erosion power index in [m^2 h].
- Total storm wave energy in [$Wh\ m^{-1}$].

Author contributions. SP and CF contributed to the design of the study. CF performed the hydrodynamic and wave numerical simulations. SP performed the data analysis and visualization. SD contributed to the analysis of the wind data. All authors contributed to the interpretation of the results. All authors reviewed and edited the manuscript. CF secured funding for the study.

Competing interests. The authors declare that they have no conflict of interest.

Acknowledgements. This study has been partially supported by the MEDICANE (Earth observations as a cornerstone to the understanding and prediction of tropical-like cyclone risk in the Mediterranean; https://medicanes.isac.cnr.it/) project funded by the European Space Agency (contract No. 4000144111/23/I-KE).

https://doi.org/10.5194/egusphere-2026-2774
Preprint. Discussion started: 16 June 2026

References

Ali, E., Cramer, W., Carnicer, J., Georgopoulou, E., Hilmi, N., Cozannet, G. L., and Lionello, P.: Cross-Chapter Paper 4: Mediterranean Region, In climate change 2022: Impacts, adaptation and vulnerability, Contribution of Working Group II to the Sixth Assessment Report of the Intergovernmental Panel on Climate Change, https://doi.org/:10.1017/9781009325844.021, 2022.

Amarouche, K. and Akpınar, A.: Increasing Trend on Storm Wave Intensity in the Western Mediterranean, Climate, 9, https://doi.org/10.3390/cli9010011, 2021.

Amarouche, K., Akpınar, A., and Semedo, A.: Wave storm events in the Western Mediterranean Sea over four decades, Ocean Modelling, 170, 101 933, https://doi.org/https://doi.org/10.1016/j.ocemod.2021.101933, 2022.

Anfuso, G., Rangel-Buitrago, N., Cortés-Useche, C., Iglesias Castillo, B., and Gracia, F.: Characterization of storm events along the Gulf of Cadiz (eastern central Atlantic Ocean), International Journal of Climatology, 36, 3690–3707, https://doi.org/https://doi.org/10.1002/joc.4585, 2016.

Arena, F., Laface, V., Malara, G., and Romolo, A.: Estimation of Downtime and of Missed Energy Associated with a Wave Energy Converter by the Equivalent Power Storm Model, Energies, 8, 11 575–11 591, https://doi.org/10.3390/en81011575, 2015.

Avolio, E., Fanelli, C., Pisano, A., and Miglietta, M. M.: Unveiling the Relationship Between Mediterranean Tropical-Like Cyclones and Rising Sea Surface Temperature, Geophysical Research Letters, 51, e2024GL109 921, https://doi.org/https://doi.org/10.1029/2024GL109921, e2024GL109921 2024GL109921, 2024.

Babagolimatikolaei, J.: The impact of Cyclone Ianos on the hydrodynamics of the Ionian Sea, Dynamics of Atmospheres and Oceans, 114, 101 673, https://doi.org/https://doi.org/10.1016/j.dynatmoce.2026.101673, 2026.

Bajo, M., Međugorac, I., Umgiesser, G., and Orlić, M.: Storm surge and seiche modelling in the Adriatic Sea and the impact of data assimilation, Quarterly Journal of the Royal Meteorological Society, 145, 2070–2084, https://doi.org/https://doi.org/10.1002/qj.3544, 2019.

Barbariol, F., Davison, S., Falcieri, F. M., Ferretti, R., Ricchi, A., Sclavo, M., and Benetazzo, A.: Wind Waves in the Mediterranean Sea: An ERA5 Reanalysis Wind-Based Climatology, Frontiers in Marine Science, Volume 8 - 2021, https://doi.org/10.3389/fmars.2021.760614, 2021.

Bellafiore, D., McKiver, W. J., Ferrarin, C., and Umgiesser, G.: The importance of modeling nonhydrostatic processes for dense water reproduction in the Southern Adriatic Sea, Ocean Modelling, 125, 22–38, https://doi.org/https://doi.org/10.1016/j.ocemod.2018.03.001, 2018.

Boccotti, P.: Wave Mechanics for Ocean Engineering, Elsevier Science, 2000.

Boyes, S. and Elliott, M.: European Challenges to Coastal Management from Storm Surges, chap. 22, pp. 339–361, John Wiley & Sons, Ltd, ISBN 9781119383567, https://doi.org/https://doi.org/10.1002/9781119383567.ch22, 2019.

Chiggiato, J., Artale, V., Durrieu de Madron, X., Schroeder, K., Taupier-Letage, I., Velaoras, D., and Vargas-Yáñez, M.: Chapter 9 - Recent changes in the Mediterranean Sea, in: Oceanography of the Mediterranean Sea, edited by Schroeder, K. and Chiggiato, J., pp. 289–334, Elsevier, ISBN 978-0-12-823692-5, https://doi.org/https://doi.org/10.1016/B978-0-12-823692-5.00008-X, 2023.

Cohn, N., Ruggiero, P., García-Medina, G., Anderson, D., Serafin, K. A., and Biel, R.: Environmental and morphologic controls on wave-induced dune response, Geomorphology, 329, 108–128, https://doi.org/https://doi.org/10.1016/j.geomorph.2018.12.023, 2019.

Conte, D. and Lionello, P.: Characteristics of large positive and negative surges in the Mediterranean Sea and their attenuation in future climate scenarios, Global and Planetary Change, 111, 159–173, https://doi.org/https://doi.org/10.1016/j.gloplacha.2013.09.006, 2013.

https://doi.org/10.5194/egusphere-2026-2774
Preprint. Discussion started: 16 June 2026

Conte, D. and Lionello, P.: Storm Surge Distribution Along the Mediterranean Coast: Characteristics and Evolution, Procedia - Social and Behavioral Sciences, 120, 110–115, https://doi.org/https://doi.org/10.1016/j.sbspro.2014.02.087, 3rd International Geography Symposium, GEOMED2013, 10-13 June 2013, Antalya, Turkey, 2014.

Cornér, J., Bouvier, C., Doiteau, B., Pantillon, F., and Sinclair, V. A.: Classification of North Atlantic and European extratropical cyclones using multiple measures of intensity, Natural Hazards and Earth System Sciences, 25, 207–229, https://doi.org/10.5194/nhess-25-207-2025, 2025.

Cover, T. M. and Thomas, J. A.: Elements of Information Theory, John Wiley & Sons, https://doi.org/10.1002/047174882X, 2006.

Di Muzio, E., Riemer, M., Fink, A. H., and Maier-Gerber, M.: Assessing the predictability of Medicanes in ECMWF ensemble forecasts using an object-based approach, Quarterly Journal of the Royal Meteorological Society, 145, 1202–1217, https://doi.org/https://doi.org/10.1002/qj.3489, 2019.

Doiteau, B., Pantillon, F., Plu, M., Descamps, L., and Rieutord, T.: Systematic evaluation of the predictability of different Mediterranean cyclone categories, Weather and Climate Dynamics, 5, 1409–1427, https://doi.org/10.5194/wcd-5-1409-2024, 2024.

Dolan, R. and Davis, R. E.: An Intensity Scale for Atlantic Coast Northeast Storms, Journal of Coastal Research, 8, 840–853, http://www.jstor.org/stable/4298040, 1992.

Dominguez, R., Fenster, M. S., and McManus, J. W.: Storm frequency, magnitude, and cumulative storm beach impact along the US east coast, Earth Surface Dynamics, 12, 1145–1163, https://doi.org/10.5194/esurf-12-1145-2024, 2024.

Donatini, L., Lupieri, G., Contento, G., Feudale, L., Pedroncini, A., and Cusati, L.: A high resolution wind&wave forecast model chain for the Mediterranean and Adriatic Sea, in: Towards Green Marine Technology and Transport, edited by Carlos Guedes Soares, Roko Dejhalla, D. P., Taylor & Francis group, 2015.

Elshinnawy, A. I. and Antolínez, J. A.: A changing wave climate in the Mediterranean Sea during 58-years using UERRA-MESCAN-SURFEX high-resolution wind fields, Ocean Engineering, 271, 113 689, https://doi.org/https://doi.org/10.1016/j.oceaneng.2023.113689, 2023.

Fedele, F. and Arena, F.: Long-Term Statistics and Extreme Waves of Sea Storms, Journal of Physical Oceanography, 40, 1106 – 1117, https://doi.org/10.1175/2009JPO4335.1, 2010.

Fenster, M. S. and Dominguez, R.: Quantifying Coastal Storm Impacts Using a New Cumulative Storm Impact Index (CSII) Model: Application Along the Virginia Coast, USA, Journal of Geophysical Research: Earth Surface, 127, e2022JF006 641, https://doi.org/https://doi.org/10.1029/2022JF006641, e2022JF006641 2022JF006641, 2022.

Ferrarin, C., Roland, A., Bajo, M., Umgiesser, G., Cucco, A., Davolio, S., Buzzi, A., Malguzzi, P., and Drofa, O.: Tide-surge-wave modelling and forecasting in the Mediterranean Sea with focus on the Italian coast, Ocean Modelling, 61, 38–48, https://doi.org/https://doi.org/10.1016/j.ocemod.2012.10.003, 2013.

Ferrarin, C., Bellafiore, D., Sannino, G., Bajo, M., and Umgiesser, G.: Tidal dynamics in the inter-connected Mediterranean, Marmara, Black and Azov seas, Progress in Oceanography, 161, 102–115, https://doi.org/https://doi.org/10.1016/j.pocean.2018.02.006, 2018.

Ferrarin, C., Davolio, S., Bellafiore, D., Ghezzo, M., Maicu, F., Kiver, W. M., Drofa, O., Umgiesser, G., Bajo, M., Pascalis, F. D., Malguzzi, P., Zaggia, L., Lorenzetti, G., and Manfè, G.: Cross-scale operational oceanography in the Adriatic Sea, Journal of Operational Oceanography, 12, 86–103, https://doi.org/10.1080/1755876X.2019.1576275, 2019.

Ferrarin, C., Penna, P., Penna, A., Spada, V., Ricci, F., Bilić, J., Krzelj, M., Ordulj, M., Šikoronja, M., Đuračić, I., Iagnemma, L., Bućan, M., Baldrighi, E., Grilli, F., Moro, F., Casabianca, S., Bolognini, L., and Marini, M.: Modelling the Quality of Bathing Waters in the Adriatic Sea, Water, 13, https://doi.org/10.3390/w13111525, 2021.

https://doi.org/10.5194/egusphere-2026-2774
Preprint. Discussion started: 16 June 2026

Ferrarin, C., Pantillon, F., Davolio, S., Bajo, M., Miglietta, M. M., Avolio, E., Carrió, D. S., Pytharoulis, I., Sanchez, C., Patlakas, P., González-Alemán, J. J., and Flaounas, E.: Assessing the coastal hazard of Medicane Ianos through ensemble modelling, Natural Hazards and Earth System Sciences, 23, 2273–2287, https://doi.org/10.5194/nhess-23-2273-2023, 2023.

Flaounas, E., Davolio, S., Raveh-Rubin, S., Pantillon, F., Miglietta, M. M., Gaertner, M. A., Hatzaki, M., Homar, V., Khodayar, S., Korres, G., Kotroni, V., Kushta, J., Reale, M., and Ricard, D.: Mediterranean cyclones: current knowledge and open questions on dynamics, prediction, climatology and impacts, Weather and Climate Dynamics, 3, 173–208, https://doi.org/10.5194/wcd-3-173-2022, 2022.

Flaounas, E., Aragão, L., Bernini, L., Dafis, S., Doiteau, B., Flocas, H., Gray, S. L., Karwat, A., Kouroutzoglou, J., Lionello, P., Miglietta, M. M., Pantillon, F., Pasquero, C., Patlakas, P., Picornell, M. A., Porcù, F., Priestley, M. D. K., Reale, M., Roberts, M. J., Saaroni, H., Sandler, D., Scoccimarro, E., Sprenger, M., and Ziv, B.: A composite approach to produce reference datasets for extratropical cyclone tracks: application to Mediterranean cyclones, Weather and Climate Dynamics, 4, 639–661, https://doi.org/10.5194/wcd-4-639-2023, 2023.

Flaounas, E., Dafis, S., Davolio, S., Faranda, D., Ferrarin, C., Hartmuth, K., Hochman, A., Koutroulis, A., Khodayar, S., Miglietta, M. M., Pantillon, F., Patlakas, P., Sprenger, M., and Thurnherr, I.: Dynamics, predictability, impacts and climate change considerations of the catastrophic Mediterranean Storm Daniel (2023), Weather and Climate Dynamics, 6, 1515–1538, https://doi.org/10.5194/wcd-6-1515-2025, 2025.

Givon, Y., Hess, O., Flaounas, E., Catto, J. L., Sprenger, M., and Raveh-Rubin, S.: Process-based classification of Mediterranean cyclones using potential vorticity, Weather and Climate Dynamics, 5, 133–162, https://doi.org/10.5194/wcd-5-133-2024, 2024.

Haigh, I. D., Marcos, M., Talke, S. A., Woodworth, P. L., Hunter, J. R., Hague, B. S., Arns, A., Bradshaw, E., and Thompson, P.: GESLA Version 3: A major update to the global higher-frequency sea-level dataset, Geoscience Data Journal, 10, 293–314, https://doi.org/https://doi.org/10.1002/gdj3.174, 2023.

Hersbach, H., Bell, B., Berrisford, P., Hirahara, S., Horányi, A., Muñoz-Sabater, J., Nicolas, J., Peubey, C., Radu, R., Schepers, D., Simmons, A., Soci, C., Abdalla, S., Abellan, X., Balsamo, G., Bechtold, P., Biavati, G., Bidlot, J., Bonavita, M., De Chiara, G., Dahlgren, P., Dee, D., Diamantakis, M., Dragani, R., Flemming, J., Forbes, R., Fuentes, M., Geer, A., Haimberger, L., Healy, S., Hogan, R. J., Hólm, E., Janisková, M., Keeley, S., Laloyaux, P., Lopez, P., Lupu, C., Radnoti, G., de Rosnay, P., Rozum, I., Vamborg, F., Villaume, S., and Thépaut, J.-N.: The ERA5 global reanalysis, Quarterly Journal of the Royal Meteorological Society, 146, 1999–2049, https://doi.org/https://doi.org/10.1002/qj.3803, 2020.

Jansa, A., Alpert, P., Arbogast, P., Buzzi, A., Ivancan-Picek, B., Kotroni, V., Llasat, M. C., Ramis, C., Richard, E., Romero, R., and Speranza, A.: MEDEX: a general overview, Natural Hazards and Earth System Sciences, 14, 1965–1984, https://doi.org/10.5194/nhess-14-1965-2014, 2014.

John A. Knaff, S. P. L. and Molenar, D. A.: An Objective Satellite-Based Tropical Cyclone Size Climatology, Journal of Climate, 27, 455–476, https://doi.org/https://doi.org/10.1175/JCLI-D-13-00096.1, 2014.

Kantha, L. H.: Barotropic tides in the global oceans from a nonlinear tidal model assimilating altimetric tides: 1. Model description and results, Journal of Geophysical Research: Oceans, 100, 25 283–25 308, https://doi.org/https://doi.org/10.1029/95JC02578, 1995.

Khodayar, S., Kushta, J., Catto, J. L., Dafis, S., Davolio, S., Ferrarin, C., Flaounas, E., Groenemeijer, P., Hatzaki, M., Hochman, A., Kotroni, V., Landa, J., Láng-Ritter, I., Lazoglou, G., Liberato, M. L. R., Miglietta, M. M., Papagiannaki, K., Patlakas, P., Stojanov, R., and Zittis, G.: Mediterranean Cyclones in a Changing Climate: A Review on Their Socio-Economic Impacts, Reviews of Geophysics, 63, e2024RG000 853, https://doi.org/https://doi.org/10.1029/2024RG000853, e2024RG000853 2024RG000853, 2025.

Komar, P. D.: Handbook of Coastal Processes and Erosion, Taylor & Francis Group, https://doi.org/doi.org/10.1201/9781351072908, 1983.

https://doi.org/10.5194/egusphere-2026-2774
Preprint. Discussion started: 16 June 2026

Laarne, P., Zaidan, M. A., and Nieminen, T.: ennemi: Non-linear correlation detection with mutual information, SoftwareX, 14, 100 686, https://doi.org/https://doi.org/10.1016/j.softx.2021.100686, 2021.

Laarne, P., Amnell, E., Zaidan, M. A., Mikkonen, S., and Nieminen, T.: Exploring Non-Linear Dependencies in Atmospheric Data with Mutual Information, Atmosphere, 13, https://doi.org/10.3390/atmos13071046, 2022.

Lagouvardos, K., Karagiannidis, A., Dafis, S., Kalimeris, A., and Kotroni, V.: Ianos—A Hurricane in the Mediterranean, Bulletin of the American Meteorological Society, 103, E1621 – E1636, https://doi.org/10.1175/BAMS-D-20-0274.1, 2022.

Leijnse, T. W. B., Giardino, A., Nederhoff, K., and Caires, S.: Generating reliable estimates of tropical-cyclone-induced coastal hazards along the Bay of Bengal for current and future climates using synthetic tracks, Natural Hazards and Earth System Sciences, 22, 1863–1891, https://doi.org/10.5194/nhess-22-1863-2022, 2022.

Lionello, P., Conte, D., Marzo, L., and Scarascia, L.: The contrasting effect of increasing mean sea level and decreasing storminess on the maximum water level during storms along the coast of the Mediterranean Sea in the mid 21st century, Global and Planetary Change, 151, 80–91, https://doi.org/https://doi.org/10.1016/j.gloplacha.2016.06.012, Climate Variability and Change in the Mediterranean Region, 2017.

Lionello, P., Conte, D., and Reale, M.: The effect of cyclones crossing the Mediterranean region on sea level anomalies on the Mediterranean Sea coast, Natural Hazards and Earth System Sciences, 19, 1541–1564, https://doi.org/10.5194/nhess-19-1541-2019, 2019.

Lionello, P., Giorgi, F., Rohling, E., and Seager, R.: Chapter 3 - Mediterranean climate: past, present and future, in: Oceanography of the Mediterranean Sea, edited by Schroeder, K. and Chiggiato, J., pp. 41–91, Elsevier, ISBN 978-0-12-823692-5, https://doi.org/https://doi.org/10.1016/B978-0-12-823692-5.00011-X, 2023.

Lira-Loarca, A., Cobos, M., Ángel Losada, M., and Baquerizo, A.: Storm characterization and simulation for damage evolution models of maritime structures, Coastal Engineering, 156, 103 620, https://doi.org/https://doi.org/10.1016/j.coastaleng.2019.103620, 2020.

Lira-Loarca, A., Cáceres-Euse, A., De-Leo, F., and Besio, G.: Wave modeling with unstructured mesh for hindcast, forecast and wave hazard applications in the Mediterranean Sea, Applied Ocean Research, 122, 103 118, https://doi.org/https://doi.org/10.1016/j.apor.2022.103118, 2022.

Makris, C. V., Tolika, K., Baltikas, V. N., Velikou, K., and Krestenitis, Y. N.: The impact of climate change on the storm surges of the Mediterranean Sea: Coastal sea level responses to deep depression atmospheric systems, Ocean Modelling, 181, 102 149, https://doi.org/https://doi.org/10.1016/j.ocemod.2022.102149, 2023.

Marcos, M., Tsimplis, M. N., and Shaw, A. G. P.: Sea level extremes in southern Europe, Journal of Geophysical Research: Oceans, 114, https://doi.org/https://doi.org/10.1029/2008JC004912, 2009.

Marcos, M., Rohmer, J., Vousdoukas, M. I., Mentaschi, L., Le Cozannet, G., and Amores, A.: Increased Extreme Coastal Water Levels Due to the Combined Action of Storm Surges and Wind Waves, Geophysical Research Letters, 46, 4356–4364, https://doi.org/https://doi.org/10.1029/2019GL082599, 2019.

Martzikos, N. T., Prinos, P. E., Memos, C. D., and Tsoukala, V. K.: Statistical analysis of Mediterranean coastal storms, Oceanologia, 63, 133–148, https://doi.org/https://doi.org/10.1016/j.oceano.2020.11.001, 2021.

Mattei, G., Di Luccio, D., Benassai, G., Anfuso, G., Budillon, G., and Aucelli, P.: Characteristics and coastal effects of a destructive marine storm in the Gulf of Naples (southern Italy), Natural Hazards and Earth System Sciences, 21, 3809–3825, https://doi.org/10.5194/nhess-21-3809-2021, 2021.

Melet, A., Meyssignac, B., Almar, R., and Cozannet, G. L.: Under-estimated wave contribution to coastal sea-level rise, Nature Climate Change, p. 234–239, https://doi.org/https://doi.org/10.1038/s41558-018-0088-y, 2018.

https://doi.org/10.5194/egusphere-2026-2774
Preprint. Discussion started: 16 June 2026

Mentaschi, L., Besio, G., Cassola, F., and Mazzino, A.: Performance evaluation of Wavewatch III in the Mediterranean Sea, Ocean Modelling, 90, 82–94, https://doi.org/https://doi.org/10.1016/j.ocemod.2015.04.003, 2015.

Miglietta, M. M., Flaounas, E., González-Alemán, J. J., Panegrossi, G., Gaertner, M. A., Pantillon, F., Pasquero, C., Schultz, D. M., D'Adderio, L. P., Dafis, S., Husson, R., Ricchi, A., Carrió, D. S. C., Davolio, S., Fita, L., Ángeles Picornell, M., Pytharoulis, I., Raveh-Rubin, S., Scoccimarro, E., Bernini, L., Cavicchia, L., Conte, D., Ferretti, R., Flocas, H., Gutiérrez-Fernández, J., Hatzaki, M., Santaner, V. H., Jansà, A., and Patlakas, P.: Defining Medicanes: Bridging the Knowledge Gap between Tropical and Extratropical Cyclones in the Mediterranean, Bulletin of the American Meteorological Society, 106, E1955 – E1971, https://doi.org/10.1175/BAMS-D-24-0289.1, 2025.

Molina, R., Manno, G., Lo Re, C., Anfuso, G., and Ciraolo, G.: Storm Energy Flux Characterization along the Mediterranean Coast of Andalusia (Spain), Water, 11, https://doi.org/10.3390/w11030509, 2019.

Ojeda, E., Appendini, C. M., and Mendoza, E. T.: Storm-wave trends in Mexican waters of the Gulf of Mexico and Caribbean Sea, Natural Hazards and Earth System Sciences, 17, 1305–1317, https://doi.org/10.5194/nhess-17-1305-2017, 2017.

Piollé, J.-F., Dodet, G., and Quilfen, Y.: ESA Sea State Climate Change Initiative (Sea_State_cci) : Global remote sensing daily merged multi-mission along-track significant wave height from altimetry, L3 product, version 3, https://doi.org/10.5285/E6AF67FCA81C40B7BB3EDDAADDE06909, 2022.

Pomaro, A., Cavaleri, L., and Lionello, P.: Climatology and trends of the Adriatic Sea wind waves: analysis of a 37-year long instrumental data set, International Journal of Climatology, 37, 4237–4250, https://doi.org/https://doi.org/10.1002/joc.5066, 2017.

Portal, A., Raveh-Rubin, S., Catto, J. L., Givon, Y., and Martius, O.: Linking compound weather extremes to Mediterranean cyclones, fronts, and airstreams, Weather and Climate Dynamics, 5, 1043–1060, https://doi.org/10.5194/wcd-5-1043-2024, 2024.

Pugh, D. and Woodworth, P.: Sea-Level Science: Understanding Tides, Surges, Tsunamis and Mean Sea-Level Changes, Cambridge University Press, 2014.

Pérez-Alarcón, A., Sorí, R., Fernández-Alvarez, J. C., Nieto, R., and Gimeno, L.: Comparative climatology of outer tropical cyclone size using radial wind profiles, Weather and Climate Extremes, 33, 100 366, https://doi.org/https://doi.org/10.1016/j.wace.2021.100366, 2021.

Rousseau-Rizzi, R., Raveh-Rubin, S., Catto, J. L., Portal, A., Givon, Y., and Martius, O.: A storm-relative climatology of compound hazards in Mediterranean cyclones, Weather and Climate Dynamics, 5, 1079–1101, https://doi.org/10.5194/wcd-5-1079-2024, 2024.

Scardino, G., Kushabaha, A., Miglietta, M. M., Bonaldo, D., and Scicchitano, G.: When Storms Stir the Mediterranean Depths: Chlorophyll-a Response to Mediterranean Hurricanes, EGUsphere, 2025, 1–31, https://doi.org/10.5194/egusphere-2025-3260, 2025.

Schimanke, S., Ridal, M., Le Moigne, P., Berggren, L., Undén, P., Randriamampianina, R., Andrea, U., Bazile, E., Bertelsen, A., Brousseau, P., Dahlgren, P., Edvinsson, L., El Said, A., Glinton, M., Hopsch, S., Isaksson, L., Mladek, R., Olsson, E., Verrelle, A., and Wang, Z.: CERRA sub-daily regional reanalysis data for Europe on single levels from 1984 to present. Copernicus Climate Change Service (C3S) Climate Data Store (CDS), https://doi.org/10.24381/cds.622a565a (Accessed on 28-11-2025), 2021.

Scicchitano, G., Scardino, G., Monaco, C., Piscitelli, A., Milella, M., De Giosa, F., and Mastronuzzi, G.: Comparing impact effects of common storms and Medicanes along the coast of south-eastern Sicily, Marine Geology, 439, 106 556, https://doi.org/https://doi.org/10.1016/j.margeo.2021.106556, 2021.

Sánchez-Arcilla, A., Sierra, J. P., Brown, S., Casas-Prat, M., Nicholls, R. J., Lionello, P., and Conte, D.: A review of potential physical impacts on harbours in the Mediterranean Sea under climate change, Regional Environmental Change, p. 2471–2484, https://doi.org/https://doi.org/10.1007/s10113-016-0972-9, 2016.

https://doi.org/10.5194/egusphere-2026-2774
Preprint. Discussion started: 16 June 2026

Toomey, T., Amores, A., Marcos, M., and Orfila, A.: Coastal sea levels and wind-waves in the Mediterranean Sea since 1950 from a high-resolution ocean reanalysis, Frontiers in Marine Science, Volume 9 - 2022, https://doi.org/10.3389/fmars.2022.991504, 2022a.

Toomey, T., Amores, A., Marcos, M., Orfila, A., and Romero, R.: Coastal Hazards of Tropical-Like Cyclones Over the Mediterranean Sea, Journal of Geophysical Research: Oceans, 127, e2021JC017 964, https://doi.org/https://doi.org/10.1029/2021JC017964, e2021JC017964 2021JC017964, 2022b.

Trigo, I. F., Bigg, G. R., and Davies, T. D.: Climatology of Cyclogenesis Mechanisms in the Mediterranean, Monthly Weather Review, 130, 549 – 569, https://doi.org/10.1175/1520-0493(2002)130<0549:COCMIT>2.0.CO;2, 2002.

Tuel, A. and Elthair, E.: Why Is the Mediterranean a Climate Change Hot Spot?, Journal of Climate, 33, 5829–5843, https://doi.org/10.1175/JCLI-D-19-0910.1, 2020.

Umgiesser, G., Ferrarin, C., Bajo, M., Bellafiore, D., Cucco, A., De Pascalis, F., Ghezzo, M., McKiver, W., and Arpaia, L.: Hydrodynamic modelling in marginal and coastal seas — The case of the Adriatic Sea as a permanent laboratory for numerical approach, Ocean Modelling, 179, 102 123, https://doi.org/https://doi.org/10.1016/j.ocemod.2022.102123, 2022.

Vannucchi, V., Taddei, S., Capecchi, V., Bendoni, M., and Brandini, C.: Dynamical Downscaling of ERA5 Data on the North-Western Mediterranean Sea: From Atmosphere to High-Resolution Coastal Wave Climate, Journal of Marine Science and Engineering, 9, https://doi.org/10.3390/jmse9020208, 2021.

[WW3DG], T. W. I. D. G.: User Manual and System Documentation of WAVEWATCH III, NOAA/NWS/NCEP/MMAB, College Park, MD, USA, version 6.07 edn., tech. Note 333, 2019.

Zhang, K., Douglas, B. C., and Leatherman, S. P.: Beach Erosion Potential for Severe Nor'easters, Journal of Coastal Research, 17, 309–321, http://www.jstor.org/stable/4300181, 2001.